Title
Exercise-induced Circulating Blood Factors Mediate the Benefits of Exercise on the Aged Brain

Permalink
https://escholarship.org/uc/item/1cz34473

Author
Horowitz, Alana Michelle

Publication Date
2020

Peer reviewed|Thesis/dissertation

Exercise-Induced Circulating Blood Factors Mediate
the Benefits of Exercise on the Aged Brain

by
Alana Horowitz

DISSERTATION
Submitted in partial satisfaction of the requirements for degree of
DOCTOR OF PHILOSOPHY

in

Biomedical Sciences

in the

GRADUATE DIVISION
of the
UNIVERSITY OF CALIFORNIA, SAN FRANCISCO

Approved:

DocuSigned by:
Dena Dubal
DF40821EE4774FD...   Dena Dubal
                                                                  Chair

DocuSigned by:
Saul Villeda
DocuSigned by:464...   Saul Villeda

Eric Verdin
DocuSigned by:45D...   Eric Verdin

a. Brack
8019548714A4420...   Andrew Brack

_____
                                                    Committee Members

To my Nana and Grandma,
whose love spans time and space

Acknowledgements

I would like to express my gratitude to the mentors, friends, and family that have supported me throughout my graduate career. To my thesis advisor, Saul Villeda: thank you for the opportunity to join your lab and learn from your wealth of knowledge and experiences. Your bold approach to science enabled me to pursue answers to the big questions contained in this dissertation, and your persistence in the face of every challenge inspired me to keep going. I will be forever grateful for the opportunity to be a member of Villeda Lab, and for the exponential personal and professional development I achieved under your mentorship.

I am also grateful to the powerhouse of scientists who served on my thesis committee: To Dena Dubal, thank you for encouraging me to think bigger than I initially planned, and for helping me build the imaginary monastery of science in which I pursued the most exciting and challenging parts of my project. To Eric Verdin, thank you for inspiring me with your passion for aging research, and pointing me toward low-risk, high-reward experiments from our very first meeting. To Andrew Brack, thank you for sharing your scientific curiosity and insights, and for the support and humor you offered during the many challenges of conducting, presenting, and publishing science.

To the Villeda Lab: This work would not have been possible without your endless support and friendship. To Geraldine Gontier, thank you for our countless impromptu mentorship sessions. Among many other things, you taught me to be a more outspoken and

Contributions

A.M.H., X.F. and S.A.V. developed concept and designed experiments. A.M.H. and X.F. collected and analyzed data. A.M.H. performed plasma administration and Gpld1 studies. X.F. performed plasma administration studies. G.B assisted with Gpld1 studies. L.K.S. assisted with biochemical analysis. C.I.S, A.B.S., and G.G. assisted with molecular and cognitive analysis. K.B.C. and J.H.K. provided human samples. K.W. performed mass spectrometry analysis. A.M.H. and S.A.V wrote manuscript. S.A.V supervised all aspects of this project.

Exercise-Induced Circulating Blood Factors Mediate

the Benefits of Exercise on the Aged Brain

Alana Horowitz

Abstract

Aging is associated with cognitive decline in otherwise healthy older adults. As human lifespan increases, a larger portion of the population is thus at risk for impaired cognition. This highlights the need for therapeutic approaches that restore functionality to the aged brain. The ability to reverse brain aging through systemic interventions such as exercise could provide a unique therapeutic approach to mitigate this vulnerability to cognitive decline. While exercise has long been reported to rejuvenate the aged brain, identification of therapeutic targets by which to transfer such benefits remains elusive. Work by our lab and others has demonstrated that complementary systemic manipulations, such as heterochronic parabiosis (in which the circulatory systems of young and old animals are joined), function through blood-borne factors to rejuvenate regenerative and cognitive capacity in aged mice. Given parallels between the effects of exercise and heterochronic parabiosis, we hypothesized that exercise-induced circulating blood factors could confer the benefits of exercise to the aged brain. Here, we report that circulating factors in blood plasma transfer the rejuvenating effects of exercise on adult neurogenesis and cognitive function to aged mice. We demonstrate that exercise modulates the circulating factors present in blood plasma, and that administration of exercise plasma into sedentary aged mice enhances neurogenesis and cognition. Using mature and aged mice as plasma donors, we show that circulating blood factors mediate the benefits of exercise across ages. Using mass spectrometry, we identify glycosylphosphatidylinositol specific phospholipase D1 (Gpld1) as a liver-derived, exercise-induced circulating blood factor. We demonstrate that

increasing systemic Gpld1 in aged mice ameliorates age-related regenerative and cognitive impairments by altering signaling cascades downstream of glycosylphosphatidylinositol (GPI)-anchored substrate cleavage in the aging systemic milieu. Further, we confirm that the enzymatic activity of Gpld1 directly mediates its effects on adult neurogenesis and cognitive function. Altogether, our data identify a liver-brain rejuvenation axis by which blood-based interventions can transfer the benefits of exercise to the aged brain.

Table of Contents

List of Figures

List of Tables

List of Abbreviations

BrdU   5-Bromo-2-Deoxyuridine

Serpina1a   Alpha-1-antitrypsin 1-1

Serpina1d   Alpha-1-antitrypsin 1-4

BDNF   Brain derived neurotrophic factor

CR   Caloric restriction

CREB   cAMP response element binding protein

Ca2   Carbonic anhydrase 2

Bche   Cholinesterase

CSF2   Colony stimulating factor 2

CA   Cornu Ammonis

DG   Dentate gyrus

Dcx   Doublecortin

Fndc5   Fibronectin type 5 domain containing protein

GFAP   Glial fibrillary acidic protein

Gpx3   Glutathione peroxidase 3

Gpld1   Glycosylphosphatidylinositol specific phospholipase D1

GFP   Green fluorescent protein

GDF11   Growth differentiation factor 11

HiBiT   High affinity nanoluciferase binary technology

HDTVI   Hydrodynamic tail vein injection

Ica   Inhibitor of carbonic anhydrase

Itih2   Inter-alpha-trypsin inhibitor heavy chain H2

LTP   Long term potentiation

Mbl2	Mannose binding protein C
Napsa	Napsin A
NPC	Neural progenitor cells
NSC	Neural stem cells
NOR	Novel object recognition task
Pltp	Phospholipid transfer protein
Plg	Plasminogen
RAWM	Radial Arm Water Maze
Pon1	Serum paraoxonase 1
Sox2	Sex determining region Y box 2
Tmp2	Tissue inhibitor of metalloproteinases 2
uPAR	Urokinase-type plasminogen activator receptor
Vtn	Vitronectin

Introduction

Aging is accompanied by a series of cellular and functional impairments that collectively drive vulnerability to disease. Organismal aging is broadly associated with global "hallmarks of aging" across all tissues in the body, such as stem cell dysfunction, genomic and protein instability, and altered intracellular communication, to name a few(1). In the brain, these age-related impairments drive susceptibility to dementia-related neurodegenerative disease. As brain aging occurs on a background of organismal-level functional decline, developing interventions to counteract this vulnerability in the aged brain will benefit from a more systemic approach. The need for therapeutic interventions for neurodegenerative disease is becoming more critical as our population ages. In the United States alone, the proportion of the population over the age of 65 is expected to increase from 15% to 24% of the population by 2060 (2). While this increase in lifespan represents significant scientific and medical progress, it has also been accompanied by a drastic rise in age-associated disease. For example, Alzheimer's disease, one of multiple dementia-related neurodegenerative diseases primarily seen in adults over the age of 65, affected 5 million people in 2013 and is predicted to affect 14 million by 2050 in the United States(3). Beyond the personal cost of living with dementia-related neurodegenerative diseases, the monetary cost to society is in the billions. Thus, while longer lifespan indicates successful scientific and medical progress, it requires a corresponding increase in healthspan, the years lived free from disease, to prove truly transformative for human quality of life. The capacity to rejuvenate the aged brain is emerging as a tantalizing prospect for the treatment of dementia-related neurodegenerative diseases of aging(4). Results from animal studies involving systemic interventions that promote healthspan— including exposure to a young systemic environment or exercise—demonstrate the rejuvenation of

regenerative and functional capacity in aged tissues (**Figure 1.1**). It is now evident that such rejuvenation even extends to the aged brain at the regenerative, functional, and cognitive level. Therefore, the application of proven systemic interventions that extend healthspan may prove key in our ability to restore function to the aging brain to prevent onset, or even counteract the progression, of dementia-related neurodegenerative disease in the elderly. This dissertation explores the role of systemic, circulating factors in mediating the beneficial effects of exercise on the aged brain, and the potential to apply those factors to therapeutic effect.

The Aging Hippocampus

The Hippocampal Formation

The hippocampus is a brain region that is particularly vulnerable to the effects of aging. It consists of a tri-synaptic circuit of distinct sub-regions responsible for processing sensory information to enable spatial and episodic learning and memory(*5*). The major input to the tri-synaptic circuit is the entorhinal cortex, from which sensory information is conveyed along the perforant path to dentate gyrus (DG) granule cells. This initiates an excitatory signaling cascade, which progresses through the Cornu Ammonis (CA) regions of the hippocampus. Specifically, the DG projects mossy fibers to the CA3 pyramidal cells, which further conveys the signal via Schaffer collaterals to the CA1. Closing the circuit, CA1 axons project back to the entorhinal cortex directly and through the subiculum. Among this central neuronal circuit exists an array of inhibitory neurons, developing newborn neurons, astrocytes, microglia, and the complex neurovasculature. Altogether, these cells make up the complex structure of the hippocampus.

Hippocampal-Dependent Cognition

This structure underlies the major function of the hippocampus: to enable spatial and episodic learning and memory. Spatial memory refers to recollection of information about orientation in the environment, whereas episodic memory is the recollection of a specific event, tied to a time and place(*6*). Activity-dependent changes in the strength of synaptic connections between neurons in the hippocampal circuit, referred to as synaptic plasticity, is thought to underlie this capacity for learning and memory(*7*). Synaptic plasticity enables the hippocampus to process environmental information, record it, and transfer it to long-term storage via specific ensembles of activated neurons(*5*).

Hippocampal dependent learning and memory is evaluated using a wide array of cognitive tasks in model organisms and humans. In mice, these tasks can be used to evaluate spatial learning and memory, recognition memory, and associative memory, among others. Variations in the memory type tested are dependent on the task design and latency between training and testing. Spatial learning and memory can be assessed with Y-Maze and Radial Arm Water Maze (RAWM) tasks. The simpler of the two is the Y-Maze, a 3-arm maze that relies on the inherent exploratory nature of mice, in which mice that recall previously explored arms will display bias to the novel arm. RAWM is more complex, requiring mice to recall the location of an escape platform among 6-8 potential locations. Recognition memory can be tested with the novel object recognition task (NOR), which tests the ability to recognize an object that was previously encountered. Associative memory is predominantly tested using fear conditioning, in which mice learn to predict an aversive stimulus associated with a specific context or cue. Altogether, these tasks and others enable the evaluation of multiple types of hippocampal-dependent learning and memory. Evidence for the necessity of the hippocampus in these tasks is supported by studies using pharmacologic and molecular manipulations(*8*).

Adult Hippocampal Neurogenesis

The hippocampus is one of the two major sites of neurogenesis in the adult brain(*9*, *10*). Here, neural stem cells (NSCs) reside in a specialized neurogenic niche, where they proliferate and differentiate to ultimately produce new excitatory granule cells in the dentate gyrus (DG) of the hippocampus(*11*). The production of new granule cells relies on the generation of highly proliferative neural progenitor cells (NPCs) from NSCs. These neuronal lineage-restricted cells differentiate into neuroblasts, which ultimately migrate into the granule cell layer and transition into post-mitotic immature neurons(*12*). Newborn neurons fully integrate into existing circuitry about four weeks post-birth. Study of these cells has yielded reliable markers by which researchers can assess cell number and function throughout the neurogenic cascade in mice. The process is highly regulated by cell-intrinsic and extrinsic processes(*13*). Cell-intrinsic factors include transcriptional, epigenetic, and cell-cycle regulators such as FoxO, Tet2, and p16 (*14-16*). Extrinsic factors are more broad-ranging, as they can originate from the niche or systemic environment. Within the hippocampal niche, growth factors, neurotransmitters, and hormones can influence NSC activation, proliferation, and maturation(*17*). For example, the brain derived neurotrophic factor (BDNF) is well-known growth factor that increases the proliferation and maturation of newborn neurons(*18*). Outside of the niche, systemic and environmental factors such as exercise, environmental enrichment, learning, and young blood exposure can increase neurogenesis(*19*). In contrast, pathological systemic influences, such as stress, diabetes, and aging can impair neurogenesis(*20-22*).

It is well appreciated that neurogenesis persists throughout life in model organisms, such as mice; however, the persistence of neurogenesis in the adult human hippocampus has recently been called into question(*23*). Previous and subsequent studies offer an abundance of support for the existence of adult neurogenesis in the human brain. These studies employ a wide variety of approaches, including 5-Bromo-2-Deoxyuridine (BrdU) birth-dating, carbon

dating, and histological approaches to demonstrate adult hippocampal neurogenesis in humans into the ninth decade of life (*24-28*).

Hippocampal Aging

Major hallmarks of hippocampal aging include decreased regenerative capacity, altered vasculature, increased neuroinflammation, and impairments in synaptic plasticity that culminate in cognitive dysfunction (*29-31*). Regenerative capacity in the brain precipitously declines with age(*32-34*). This decline in neurogenesis can be observed across the neurogenic cascade, including fewer cells at all stages of differentiation and lower levels of NSC activation and NPC proliferation(*35*).

Neurogenesis is tightly linked to nutritive sources provided by the cerebrovasculature through the blood–brain barrier, an anatomical separation between the central nervous system and the periphery consisting of the vascular cells and glia. With age, cerebral blood flow and blood–brain barrier integrity also decline, compromising metabolic support for neurogenesis and proper neuronal signaling and promoting inflammatory responses by resident immune cells(*36, 37*). Correspondingly, increased activation of astrocytes and microglia underlies the neuroinflammatory hallmark of brain aging, accompanied by increased pro-inflammatory cytokine production(*38*). Such pro-inflammatory changes have now been shown to contribute to vulnerability and advancement of cognitive decline through processes such as accumulation of complement factors (a component of innate immunity) in microglia(*38, 39*).

Synaptic plasticity in mature neurons also declines with age(*40*). Structurally, the age-related decrease in synaptic density, manifesting as fewer numbers of dendritic spines, reduces the capacity for neurons to receive signals from neighboring axons(*41, 42*). Aged neurons have further deficits in synaptic-plasticity related protein expression, activity dependent immediate early gene activation, as well as long-term potentiation and long-term depression(*43-45*).

Consistent with this high level of cellular dysfunction, cognitive processes such as learning and memory also decline with age.

The Link between Neurogenesis and Cognition

Owing to known associations between adult neurogenesis and cognitive function, age-related loss in regenerative capacity has been proposed to contribute to cognitive decline, although the direct link between the two processes in the context of aging has yet to be resolved(*46*, *47*). The connection was first demonstrated via correlations, in which levels of neurogenesis in aged rats predicted spatial memory performance in water maze(*46*). Further, the precipitous age-related decline in neurogenesis correlates with overall cognitive decline(*32*). Accumulating evidence now suggests a unique role for neurogenesis in specific cognitive processes. This role is reliant on the unique properties of newborn neurons, including increased sensitivity to neurotransmitters and lower induction thresholds(*48*, *49*). These characteristics enable newborn neurons to be preferentially integrated into spatial memory networks in the dentate gyrus(*50*). In line with these findings, stimulating adult neurogenesis is sufficient to increase pattern separation performance in mice(*51*). Similarly, decreasing adult neurogenesis or inhibiting newborn neurons via optogenetic and pharmacological interventions is sufficient to impair learning and memory in adult mice during spatial learning and pattern separation tasks(*52-54*). These data support the idea that the maturation and integration of newborn neurons contributes to hippocampal-dependent learning and memory(*55*, *56*).

Systemic Brain Rejuvenation Strategies

The age-related decline in both neurogenesis and cognition is amenable to systemic interventions(*57*). Indeed, systemically mediated rejuvenating interventions such as caloric restriction (CR; a reduction in caloric intake without malnutrition), exercise, and heterochronic parabiosis (in which the circulatory systems of a young and old animal are joined) have succeeded in rejuvenating aged tissues, including the brain, to improve organismal healthspan (*58-69*). Exercise, for example, enhances neurogenesis and improves cognition at old age(*70*, *71*). The effectiveness of these interventions suggests a systemic mechanism by which age-related regenerative and cognitive decline can be slowed, or possibly even reversed.

Caloric Restriction

The most robust and reliably replicated systemic intervention to improve lifespan and/or healthspan in rodents and non-human primates is CR(*67*, *72*). In primates, CR has proved to be protective against many facets of aging, including gray matter loss in the brain(*66*). In rodent models, CR leads to beneficial metabolic changes, protection from oxidative stress, neurotrophic factor production, increased autophagy, and neurogenesis(*73-76*). CR also promotes the maintenance of cerebral blood flow and white matter integrity with age(*77*, *78*). While CR has been demonstrated to improve spatial learning and memory in aged mice(*78*), global effects on cognition remain unresolved, as CR has failed to improve other hippocampal-dependent cognitive processes(*79-81*). It is suggested that such inconsistent results could be due to the varied macronutrient ratios in CR regimes, the age of CR onset, and the metabolic heterogeneity of the diverse cell types in the hippocampus(*82-84*). Nevertheless, CR reliably improves overall organismal healthspan and likewise improves behavioral and cognitive metrics in animal models of neurodegenerative disease(*85*, *86*). While the potential benefits of CR for human healthspan are evident, limitations of feasibility, adequate health monitoring, and

adherence remain. Indeed, in a long-term CR study conducted by the CALERIE Research Group, low adherence decreased the average caloric deficit from the anticipated 25% to 11.7% over a 2-year period, offsetting major expected beneficial metabolic outcomes[87]. Consequently, limits to the application of CR need to be further addressed before widespread therapeutic application.

Heterochronic Parabiosis

The classical model of heterochronic parabiosis has recently re-emerged as an experimental platform to explore the intricate interplay between the systemic environment and organismal aging. To date, heterochronic parabiosis experiments have been used to explore the effects of aging throughout the body in tissues including muscle, pancreas, bone, heart, and brain[20, 58-61, 63, 65, 69].

Heterochronic parabiosis studies have pointed to a role for old blood in driving brain aging[20, 88, 89]. Regenerative capacity in young heterochronic parabionts is impaired, with neurogenesis decreasing the hippocampus[20, 69]. Further evidence of the pro-aging effects of old blood come from studies utilizing old blood plasma injections. Short-term systemic administration of old plasma recapitulates the effects of heterochronic parabiosis on adult neurogenesis, implicating circulating factors in the detrimental effects of old blood[90]. Long-term administration of old plasma over one month further resulted in impaired hippocampal-dependent learning and memory[20].

In contrast, the exposure of an aged mouse to a youthful systemic environment through heterochronic parabiosis rejuvenates brain function, indicating that circulating blood factors can counteract cellular and functional age-related neuronal decline[62, 69, 91]. Regenerative capacity in the hippocampus of aged heterochronic parabionts was enhanced after exposure to a young systemic environment[62, 69]. This rejuvenating potential was maintained at a cell autonomous level with neural stem cells from old heterochronic parabionts showing enhanced

8

self-renewal potential in vitro(*69*). Vascularization of the neurogenic niche is known to influence

neural stem cell function(*92, 93*), and correspondingly heterochronic parabiosis also restored

blood vessel volume in the aged subventricular zone neurogenic niche to youthful levels(*69*).

Beyond regenerative function, exposure to a young systemic environment also enhanced

synaptic plasticity, eliciting an increase in the expression of immediate early genes and the

density of dendritic spines as well as enhancements in long term potentiation (LTP)(*62*). At a

cognitive level, long-term administration of young plasma over one month was sufficient to

reverse cognitive impairments in hippocampal-dependent learning and memory in old mice

through increased activation of the transcription factor cAMP response element binding protein

(CREB)(*62*). Consistently, old heterochronic parabionts that were separated from their young

partner also demonstrated improvements in their olfactory discrimination ability compared to

separated old isochronic controls. In a pre-clinical experiment, human umbilical cord-blood-

derived plasma was demonstrated to similarly enhance immediate early gene expression,

increase LTP, and improve cognitive function in aged mice(*94*). This demonstration of the

rejuvenating potential of human umbilical cord blood in mice strengthens the possibility that

human blood can also be used to elicit brain rejuvenation in humans. Thus far, growth

differentiation factor 11 (GDF11), colony stimulating factor 2 (CSF2), and tissue inhibitor of

metalloproteinases 2 (TIMP2) have been identified as rejuvenating factors in young adult and/or

juvenile blood(*58, 94*). While its role in cardiac and skeletal muscle rejuvenation is currently

under discussion(*58, 61, 95*), GDF11 was demonstrated to enhance neurogenesis and cerebral

blood flow in aged mice when systemically administered(*69*). Hinting at the multifactorial nature

of young plasma, TIMP2 or CSF2 administration was also shown to enhance immediate early

gene expression, LTP, and cognitive performance in aged mice(*94*). Despite their shared

rejuvenating effects, GDF11 was identified in young adult mouse plasma, while TIMP2 and

CSF2 were identified in human umbilical cord blood, a comparatively early developmental

stage. These distinctions again point to the importance of kinetics in determining circulating

factor changes. As more insight into the rejuvenating potential of young blood is obtained, it becomes evident that research is necessary to identify a breadth of factors by which to reverse global hallmarks of brain aging.

Exercise

Robust benefits of exercise have also been consistently observed to increase healthspan, although its role in extending lifespan in mice remains obfuscated(*68*, *96*, *97*). Exercise has been shown to improve a wide range of age-related cellular and functional impairments throughout the body. For example, frailty, which refers to a global decline in function that encompasses grip strength, activity, overall energy, and unintentional weight loss, is amenable to the effects of exercise(*37*, *97*, *98*). In rodent models, exercise reduces age-associated frailty through increasing skeletal muscle function(*97*) and has been shown to improve grip strength and nesting and burrowing behaviors even when initiated at middle age(*37*). In the normal aged brain, exercise has been shown to enhance regenerative capacity by promoting hippocampal neurogenesis, effects that correlated with improved learning and memory(*70*). Furthermore, exercise also improved broad cellular hallmarks of brain aging in aged mice, including increased synaptic plasticity, improved neurovascular integrity, and decreased microglia activation(*37*, *99*, *100*). In the context of neurodegenerative disease, researchers have utilized mouse models of Alzheimer's disease to demonstrate that exercise is able to suppress inflammatory cytokines, increase the expression of antioxidant enzymes, improve synaptic function in the hippocampus, and enhance hippocampal-dependent learning and memory (*141*). Researchers have further explored the relationship between physical exercise, healthspan, and cognitive function in human populations. Epidemiological studies demonstrate that physical activity is associated with better overall survival and function in older adults compared to their sedentary counterparts(*101*, *102*). It has been proposed that such benefits in elderly humans may be the result of counteracting muscle weakness and frailty as well as reducing circulating inflammatory

markers(*103*, *104*), consistent with animal studies. Exercise is also reported to reduce the risk of mild cognitive impairment later in life(*105-108*). From a neurodegenerative disease perspective, a 6-month program of physical exercise in adults over the age of 50 years who are at risk for Alzheimer's disease also showed significantly improved cognition over an 18-month follow-up period(*109*). While the potential for human application exists, limitations should be noted, with evidence in humans indicating that the perception of physical frailty or poor health alone can decrease adherence in the elderly(*110*). Notwithstanding, these studies point to the capacity of exercise to extend healthspan and rejuvenate cellular and functional hallmarks of brain aging, with direct relevance to neurodegenerative diseases, such as Alzheimer's disease. Despite the evident potential of exercise, its therapeutic application is limited by technical barriers in the elderly, making it critical to elucidate how exercise slows dysfunction in the aging brain(*110*).

Parallels between the benefits exposure to young blood and exercise raise the possibility that similar circulating factor mechanisms mediate such rejuvenating effects. To date, potential mechanisms, such as elevated growth factor levels, have been proposed to explain the benefits of exercise(*111-115*). In young mice, scavenging circulating growth factors, including vascular endothelial growth factor (VEGF) and insulin-like growth factor 1 (IGF1), prevents exercise-induced cognitive benefits(*113*, *115*, *116*). Similarly, limiting local growth factor signaling in the hippocampus, such as for BDNF, blocks the benefits of exercise(*112*, *117*). However, evidence is limited that these factors are sufficient to mimic the effects of exercise, and their roles have yet to be tested in the context of normal aging. For example, hippocampal over-expression of BDNF is insufficient to increase neurogenesis or cognition in Alzheimer's model mice(*118*). Alternatively, muscle- and liver-derived factors have been proposed to mediate the effects of exercise(*111*, *119*, *120*). These factors include fibronectin type 5 domain containing protein (Fndc5), Cathepsin B, B-hydroxybutryate, and platelet factor 4 (*111*, *119-122*). These data identify exercise as a rejuvenating intervention, and point to a systemic mechanism mediating its beneficial effects.
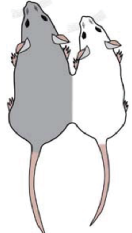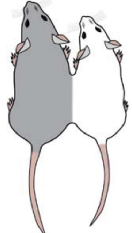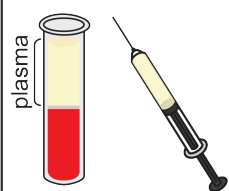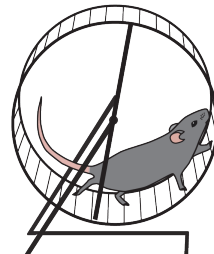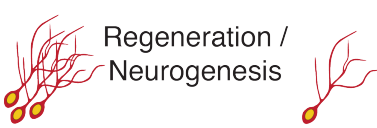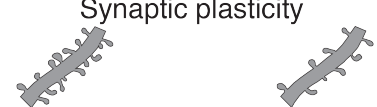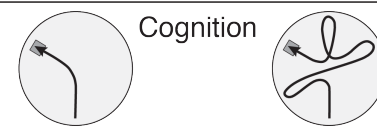
Figure 1.1. Systemic brain rejuvenation strategies. Hallmarks of hippocampal aging amenable to rejuvenation (left panel) include decreased regenerative capacity (neurogenesis), impaired synaptic plasticity, and impaired cognitive function. Systemic interventions (top panel), such as heterochronic parabiosis, young blood plasma administration, and exercise have been shown to rejuvenate hallmarks of brain aging. Cellular or functional rejuvenation elicited by systemic interventions is denoted by a check (✔) and yet-to-be-determined effects are denoted by a question mark (?).

Materials and Methods

Animal Models

The following mouse lines were used: C57BL/6 aged mice (The Jackson Laboratory), C57BL/6 aged mice (National Institutes of Aging), and C57BL/6 mature and aged mice (Taconic Biosciences). All studies were performed with male mice. The numbers of mice used to result in statistically significant differences was calculated using standard power calculations with $\alpha = 0.05$ and a power of 0.8. We used an online tool (http://www.stat.uiowa.edu/~rlenth/Power/index.html) to calculate power and samples size based on experience with the respective tests, variability of the assays and inter-individual differences within groups. The summary table below lists each experiment with experimenter, mouse strain, and location of behavioral testing. Within each individual experiment animals from the same strain and vendor that were aged together were utilized. All animals from Taconic and Jackson were acquired at 2 months of age and aged in-house for the duration of their life. Animals are moved to a new location for behavioral assessment. The two locations where we conducted behavior are on the UCSF Parnassus campus: the UCSF Rehabilitation Behavior Core and the Villeda Lab Behavioral Suite. Mice were housed under specific pathogen-free conditions under a 12 h light-dark cycle and all animal handling and use was in accordance with institutional guidelines approved by the University of California San Francisco IACUC.

Table 2.1. Mouse strain, experimenter, and experiment locations

Experiment	Experimenter	Strain	Behavior Location
1A	AMH	C57/Bl6 TAC	UCSF Core
1B-H	AMH	C57/Bl6 TAC	UCSF Core
2A; 4D,F; S5A-B	XF, KEW	C57/Bl6 TAC	N/A
2C-F	LKS, AMH	C57/Bl6 TAC	UCSF Core
3A-K	AMH	C57/Bl6 TAC	Villeda Lab
4A-C, E	AMH	C57/Bl6 JAX	N/A
5B-H	AMH	C57/Bl6 TAC	Villeda Lab
S1A	AMH	C57/Bl6 JAX	N/A
S1B-C	CSD	C57/Bl6 NIA	Villeda Lab
S1D	ABS	C57/Bl6 JAX	Villeda Lab
S1E-G	CSD	C57/Bl6 JAX	UCSF Core
S2B-C	AMH	C57/Bl6 TAC	UCSF Core
S2D-H	XF	C57/Bl6 TAC	UCSF Core
S3B-C; F-H	XF	C57/Bl6 TAC	UCSF Core
S3D-E	AMH	C57/Bl6 TAC	UCSF Core
S4A-B	AMH, XF	C57/Bl6 TAC	N/A
S6A-J	AMH, GG	C57/Bl6 TAC	N/A
S7A-B	AMH	C57/Bl6 JAX	Villeda Lab
S7C-F	ABS	C57/Bl6 JAX	Villeda Lab
S8B-C	AMH	C57/Bl6 JAX	N/A

Animal Exercise

Exercised mice were single-housed and given continuous access to a running wheel (Cat# ENV-047, Med Associates, Inc.) in their cage for 42 days. Distance ran per mouse was tracked using Wheel Manager software (Med Associates, Inc.). Mice evaluated in behavior assays had continuous access to running wheels for full duration of experiments. Sedentary mice were single-housed and give a house and nestlet as alternative enrichment.

Animal Plasma Collection and Administration

Mouse plasma was collected by intracardial bleed at time of sacrifice from 30 mature exercised, 30 mature sedentary, 30 aged exercised, and 30 aged sedentary mice. Plasma was

prepared from blood collected with EDTA followed by centrifugation at 1000 X g. Plasma was maintained from individual mice for western blot analysis and mass spectrometry, or pooled for plasma administration. Plasma was aliquoted stored at -80ºC until use. Prior to administration plasma was dialyzed using 3.5-kDa D-tube dialyzers (EMD Millipore) in PBS to remove EDTA. Aged mice were systemically treated with plasma (100ul/injection) isolated from mature exercised, mature sedentary, aged exercised, or aged sedentary mice via intravenous tail vein injection 8 times over 24 days.

BrdU Administration

For BrdU labeling, 50mg/kg of BrdU (Sigma-Aldrich) was injected into mice intraperitoneally once a day for 5 days.

Hydrodynamic Tail Vein Injection

Hydrodynamic tail vein injections were performed as previously described(*123*). Endotoxin-free plasmids were prepared using the Qiagen Maxi-Prep Plus Kit (Cat# 12963, VWR). GPLD1 or GFP plasmid DNA (50ug) was suspended in 3mL saline and injected in the tail vein in 5-7 seconds in aged mice.

Radial Arm Water Maze

Spatial learning and memory was assessed using the radial arm water maze (RAWM) paradigm according to established protocol(*124*). In this task, the mouse is trained to the location of a constant goal arm throughout the training and testing phase. The start arm changes each trial. Entry into an incorrect arm is scored as an error, and errors are averaged over training blocks (three consecutive trials). During training (day 1), mice are trained for 12 trails (blocks 1-4), with trials alternating between a visible and hidden platform. Following an hour break, learning is tested

for 3 trials (block 5) using only a hidden platform. During testing (day 2), mice are tested for 15 trials (blocks 6-10) with a hidden platform. Investigators were blinded to treatment when scoring.

Contextual Fear Conditioning

In this task, mice learned to associate the environmental context (fear conditioning chamber) with an aversive stimulus (mild foot shock; unconditioned stimulus, US) enabling testing for hippocampal- dependent contextual fear conditioning. To assess amygdala-dependent cued fear conditioning, the mild foot shock was paired with a light and tone cue (conditioned stimulus, CS). Freezing behavior was used as a readout of conditioned fear. Specific training parameters are as follows: tone duration is 30 seconds; level is 70 dB, 2 kHz; shock duration is 2 seconds; intensity is 0.6 mA. This intensity is not painful and can easily be tolerated but will generate an unpleasant feeling. On the training day (day 1), each mouse was placed in a fear-conditioning chamber and allowed to explore for 2 min before delivery of a 30-second tone (70 dB) and light, ending with a 2-second foot shock (0.6 mA). Two minutes later, a second CS-US pair was delivered. On the testing day (day 2), each mouse was first placed in the fear-conditioning chamber containing the same exact context, but with no CS or foot shock. Freezing was analyzed for 1–2 minutes. One hour later, the mice were placed in a new context containing a different odor, cleaning solution, floor texture, chamber walls and shape. Animals could explore for 2 minutes before being re-exposed to the CS. Freezing was analyzed for 1–3 minutes using a FreezeScan video tracking system and software (Cleversys, Inc).

Y Maze

The Y Maze task was conducted using an established forced alternation protocol(*125*). During the training phase, mice were placed in the start arm facing the wall and allowed to explore the start and trained arm for 5 minutes, while entry to the 3rd arm (novel arm) was blocked. The

maze was cleaned between each mouse to remove odor cues, and the trained arm was alternated between mice. The mouse was then removed to its home cage. After 30 minutes, the block was removed and the mouse was returned to the start arm and allowed to explore all 3 arms for 5 minutes. Time spent in each arm was quantified using the Smart Video Tracking Software (Panlab; Harvard Apparatus). Percent time in each arm was defined as time in arm divided by time spent in all arms during the first minute of the task.

Novel Object Recognition

The novel object recognition task was adapted from a previously described protocol(*126*). During the habituation phase (day 1), mice could freely explore an empty arena for 10 minutes. During the training phase (day 2), two identical objects were placed in the habituated arena, and mice could explore the objects for 5 minutes. For the testing phase (day 3), one object was replaced with a novel object, and mice could explore the objects for 5 minutes. Time spent exploring each object was quantified using the Smart Video Tracking Software (Panlab; Harvard Apparatus). Two different sets of objects are used. To control for any inherent object preference, half of the mice are exposed to object A as their novel object and half to object B. To control for any potential object-independent location preference, the location of the novel object relative to the trained object is also varied. The objects were chosen based on their ability to capture the animal's interest, independent of genetic background or age. To determine percent time with novel object, we calculate (Time with novel object)/(Time with Trained Object + Time with Novel Object) * 100(*50*). In this preference index, 100% indicates full preference for the novel object, and 0% indicates full preference for the trained object. A mouse with a value of 50% would have spent equal time exploring both objects. Mice that did not explore both objects during the training phase were excluded from analysis.

Immunohistochemistry

Tissue processing and immunohistochemistry was performed on free-floating sections following standard published techniques(*88*). Mice were anesthetized with 87.5 mg/kg ketamine and 12.5mg/kg xylazine and transcardially perfused with phosphate buffered saline. Brains were removed and fixed in phosphate-buffered 4% paraformaldehyde, pH 7.4, at 4C for 48h before cryprotection with 30% sucrose. Brains were sectioned coronally at 40um with a cryomicrotime (Leica Camera, Inc.). Free floating coronal sections (40 μm) were incubated overnight with goat anti-DCX (1:7500, Santa Cruz), mouse anti-NeuN (1:1000, Millipore), rat anti-BrdU (1:1000, Abcam), goat anti-Sox2 (1:200, Santa Cruz), and rabbit anti-GFAP (1:1000, Dako) primary antibodies. Staining was revealed using fluorescent-conjugated secondary antibodies (Life Technologies). For BrdU labeling, brain sections were pre-treated with 2 N HCl at 37 C for 20 min and washed with Tris-buffered saline with Tween (TBST) before primary antibody incubation. Sections were imaged by confocal microscope (Zeiss LSM800). Individual cell number in the dentate gyrus was quantified using ImageJ software.

RNA Extraction, cDNA Synthesis and qPCR

Total RNA was isolated using TRI Reagent (Sigma-Aldrich, cat#T9424). To quantify mRNA expression levels, equal amounts of cDNA were synthesized using the High-Capacity cDNA Reverse Transcription kit (ThermoFisher Scientific, Cat# 4368813), then mixed with SYBR Fast mix (Kapa Biosystems) and primers. GAPDH or actin mRNA was amplified as an internal control. Quantitative RT-PCR was carried out in a CFX384 Real Time System (Bio-Rad).

Western Blot Analysis

Mouse hippocampi were dissected after perfusion, snap frozen and lysed in RIPA lysis buffer (Cat# ab156034, Abcam) with complete protease inhibitor (Cat# 4693116001, Sigma-Aldrich) and phosphatase inhibitor (Cat# 78420, Thermo-Fisher). Tissue lysates or plasma were mixed with 4x NuPage LDS loading buffer (Cat# NP0008, Invitrogen), loaded on a 4-12% SDS polyacrylamide gradient gel (Invitrogen) and transferred onto a nitrocellulose membrane. Equal loading of plasma was confirmed using Ponceau S solution (Cat# P7170, Sigma-Aldrich). The blots were blocked in 5% milk in Tris-Buffered Saline with Tween (TBST) and incubated with mouse anti-Tubulin B 3 (1:5000, BioLegend), rabbit anti-B-actin (1:1000, Sigma-Aldrich), rabbit anti-BDNF (1:750, Invitrogen), rabbit anti-GPLD1 (1:500, Aviva Systems Biology), rabbit anti-vitronectin (1:500, Molecular Innovations), and rabbit anti-plasminogen (1:1000, Abcam). Horseradish peroxidase-conjugated secondary antibodies and an ECL kit (GE Healthcare) were used to detect protein signals. Membranes were imaged with the ChemiDoc System (BioRad). Selected images were exported and quantified using ImageJ software (Version 2.0.0). Tubulin bands were used for normalization.

Mass Spectrometry

For proteomic analysis of exercise plasma, plasma was collected from mature and aged exercised and sedentary mice. Plasma from two mice was pooled for each condition, in duplicate, for a total of 8 samples. Samples were depleted of the most abundant proteins using a MARS3-mouse immunoaffinity column (Agilent) and desalted using Zeba columns (Pierce). Protein concentration was determined using the BCA assay (Pierce). Plasma proteins (50 ug) were digested with trypsin and labeled with iTRAQ 8plex reagent (Applied Biosystems) as previously described(*127*). Peptides were first separated offline into 18 fractions using alkaline pH reversed-phase HPLC(*128*). Peptides from each fraction were separated using a nanoLC Ultra 2D Plus

system (SCIEX) interfaced with a 5600 Triple TOF mass spectrometer (SCIEX). The peptides were initially loaded onto a guard column (300 μm i.d. × 5 mm, 5-μm particle size, 100-Å pore size; Acclaim PepMap300 C18; Thermo-Fisher) and were washed with the aqueous loading solvent that consisted of 2% solvent B [98% acetonitrile (ACN)/0.1% formic acid (FA)] in solvent A (2% ACN/0.1% FA), flow rate 12 μL/min for 3 min. Then the peptides were separated on a C18 Acclaim PepMap100 column (75 μm i.d. × 150 mm, 3-mm particle size, 100-Å pore size; Thermo Fisher Scientific) heated at 40 °C with a column oven. Peptides were eluted at a flow rate of 300 nL/min with a gradient of 2–35% solvent B for 90 min. In positive ion mode, MS scans from m/z 400–1,600 were acquired followed by MS/MS scans of the 20 most abundant ions with an exclusion time of 15 s. Proteins were identified and quantified using ProteinPilot v.5.0 software and the UniProt v. 201505 database with Mus musculus specied filter and ID focus of biological modifications. iTRAQ ratios were calculated using (one of the pools of old runners, OR1) and bias correction and background subtraction were applied. Protein ratios were calculated using only ratios from the peptide spectra that were distinct to each protein or protein form, thus eliminating any masking of changes in expression caused by the sharing of peptides among proteins. A target-decoy database containing the reversed sequences of all the proteins appended to the target database was used to calculate peptide and protein FDR rates(*129*). A total of 227 proteins were detected at the 5% local FDR.

For proteomic analysis of Gpld1 HDTVI plasma, plasma was collected from aged mice 24 hours after HDTVI with either Gpld1 or GFP plasmid DNA. Plasma was collected from 3 individual mice per condition for a total of 6 samples. Samples were depleted of the most abundant proteins using Proteome Purify 2 Mouse Serum Protein Immunodepletion Resin (R&D Systems) according to the manufacturer's protocol. Depleted samples were buffer exchanged into water on a Corning Spin X 5kD molecular weight cut off spin column and quantified by Qubit fluorometry (Life Technologies). Plasma proteins (50μg) were reduced with dithiothreitol, alkylated with iodoacetamide and digested with trypsin (Promega). Individual digested samples were processed

by solid phase extraction using an Empore C18 (3M) plate under vacuum. Briefly, columns were activated (400µL 95% acetonitrile/0.1% TFA X2) and equilibrated (400µL 0.1% TFA X4). Next, acidified samples were loaded and columns were washed (400µL 0.1% TFA X2). Finally, peptides were eluted (200µL 70% acetonitrile/0.1% TFA X2) and lyophilized for downstream processing. For mass spectrometry analysis, 2µg of protein per sample was analyzed by nano LC-MS/MS with a Waters NanoAcquity interfaced to a ThermoFisher Fusion Lumos mass spectrometer. Peptides were loaded on a trapping column and eluted over a 75 µm x 50cm analytical column (ThermoFisher P/N ES-803) at 300nL/min using a 3 hour reverse phase gradient. The mass spectrometer was operated in data-dependent mode, with the Orbitrap operating at 60,000 FWHM and 15,000 FWHM for MS and MS/MS respectively. The instrument was run with a 3s cycle for MS and MS/MS and APD was enabled. The data were processed with MaxQuant (version 1.6.0.13; Max Planck Institute for Biochemistry(*130*), which incorporates the Andromeda search engine. Using this program, the MS data were recalibrated, protein/peptide identification was made using the Andromeda database search engine, the database search results were filtered at the 1% protein and peptide FDR, and protein levels were quantified. The resulting MaxQuant output was further processed using Perseus (V 1.6.0.7; Max Planck Institute for Biochemistry). Proteomic analyses were conducted by the Sandler-Moore Mass Spectrometry Core Facility at the University of California, San Francisco or MS Bioworks (a fee-for-service provider). Gene ontology analysis was performed using STRING(*131*) on the top 20 up and down-regulated proteins, as sorted by p value.

Cell Culture

A Lenti-X 293T cell line was used for *in vitro* experiments. Cells were plated at a confluency of 85-90% for transfection experiments and cultured in DMEM + 10% FBS. Lipofectamine 3000 (ThermoFisher, Cat# L300015) was used as the transfection reagent. Supernatant was collected at 48 hours for downstream analysis. For enzymatic activity of Gpld1,

EF1a-Cre and Ubiquitin-Lox-stop-lox-PLAP were co-transfected with CMV-GFP, CMV-Gpld1, CMV-Gpld1-H133N, or CMV-Gpld1-H158N. An SEAP Reporter Gene Assay Kit (Abcam, Cat# 133077) was used to measure alkaline phosphatase activity in the media.

HDTVI Plasmids

RNA was isolated from adult mouse liver tissue using TRIZol reagent (Thermo Fisher Scientific, Cat# 15596026) and PureLink™ RNA Mini Kit following the manufacturer's instructions. The RNA concentration was determined via Nanodrop and RNA was reverse transcribed using the High-Capacity cDNA Reverse Transcription Kit (Thermo Fisher Scientific, Cat# 4368813) and oligo dT primers (Promega cat# C1101). The following primers were used for PCR amplification of the Gpld1 and Pon1 coding sequences and partial 3' and 5' untranslated regions (UTRs) from mouse liver cDNA: CACCGGAGTGACCATCAACTGGCA (Gpld1 forward primer); TCAAGAAAGCGGGGCTGAAT (Gpld1 reverse primer), CACCAGTGTTGCTGCACT TGTCC (Pon1 forward primer), CACTTTCGATGACGTGCGTG (Pon1 reverse primer). The Gpld1 and Pon1 ORFs were cloned into the pENTR D-TOPO vector (ThermoFisher Scientific, Cat# K240020) and sequence verified using the following primers: M13F, M13R, GGAAAGTCATCACCAAAGACGTCC (Gpld1-specific sequencing primer), CAGGGCAGCTCA CCTACAATG (Gpld1-specific sequencing primer). The coding sequences were further amplified and cloned into a mammalian expression plasmid using the restriction sites NheI and EcoRI for Gpld1 and XbaI and EcoRI for Pon1. The H133N and H158N mutations were generated using the and the QuikChange Lightning Site-directed Mutagenesis kit (Agilent cat# 210518) in combination with the following primers: H133N Primer 1 (GCTGACGTGAGCTGGAATAGCCTGGGTATTG), H133N Primer 2 (CAATACCCAGGCTATTCCAGCTCACGTCAGC), H158N Primer 1 (TACAACTCTTACTCTGACGCTAACTCGGCTGGTG) H158N Primer 2

(CACCAGCCGAGTTAGCGTCAGAGTAAGAGTTGTA). The bicistronic plasmid vectors expressed Gpld1 or Pon1 and an IRES eGFP reporter using a CMV promoter. Empty IRES eGFP constructs based on the same plasmids were used as controls. All coding plasmid sequences were verified by Sanger sequencing. Endotoxin free plasmid kits were used for plasmid preparation prior to in vivo use.

HiBiT Analysis

To detect the localization of HiBiT-tagged Gpld1 in various mouse tissues, mice were hydrodynamically injected with GFP, Gpld1, or Gpld1-HiBiT constructs. At 24 hours following HDTVI, mice were euthanized and plasma was collected by intracardial bleed. Following perfusion, hippocampus, cortex, cerebellum, and liver were dissected, snap frozen and lysed in RIPA lysis buffer (Abcam, Cat# ab156034) with complete protease inhibitor (Sigma-Aldrich, Cat# 4693116001) and phosphatase inhibitor (Cat# 78420, Thermo-Fisher). 20µg of protein from each sample was loaded in duplicate in an opaque 96 well plate (Corning, Cat# 353296). HiBiT luminescence was measured on the Cytation 5 (BioTek) using the Nano-Glo HiBiT Lytic Detection System (Promega, Cat# N3030) according to the manufacturer's instructions.

Human Participants

20 community-dwelling older adults (66-78 years; 10 F) enrolled in the observational UCSF Memory and Aging Center Hillblom Study of healthy brain aging were selected for inclusion. Inclusion criteria were: 1) no diagnosed memory or neurological condition (e.g., epilepsy, stroke), 2) no functional decline operationalized as a Clinical Dementia Rating scale of 0 (via study partner interviews), 3) blood draw at study visit, and 4) completion of physical activity monitoring for ≥2 weeks following study visit. To achieve optimal activity variability and blinded to all other outcomes, we selected participants between ages 60-80 with the highest (5 female, 5

male) and lowest (5 female, 5 male) step-counts to be included in the current study. The study was approved by the UCSF IRB on human research and all participants provided written, informed consent before enrolling. The study followed the guidelines of the Helsinki declaration. A summary table of participant characteristics is below.

Table 2.2. Summary of human participant characteristics

Mean (SD)	Total (n=20)	Low Activity (<7100 steps; n=8)	High Activity (≥7100 steps; n=12)
Age	73.7 (3.3) [range: 66.6, 78.8]	74.4 (2.6)	73.1 (3.7)
Sex, % F (n)	50% (10)	62% (5)	42% (5)
Education	18.2 (1.9) [range: 13, 20]	17.9 (2.4)	18.3 (1.7)
Fitbit Flex2 Daily Steps	8565.01 (4483.1) [range: 930.5, 16270.3]	3837.5 (1926.5)	11716.7 (2294.1)
Days monitored	31.4 (4.2) [range: 19, 39]	30.1 (4.9)	32.3 (3.6)
BMI	26.6 (5.9) [range: 19.8, 46.7]	28.8 (8.0)	24.7 (4.0)
Height (inches)	66.6 (4.9) [range: 57, 75]	66.4 (5.0)	67.1 (4.6)
Weight (lbs)	166.5 (33.0) [range: 111, 220]	177.0 (32.1)	159.3 (34.3)
Heart Rate	65.5 (8.8) [range: 48, 85]	64.8 (10.8)	66 (7.6)

Blood Pressure
     Systolic
     Diastolic
	130.9 (17.0) [range: 100-172]
	71.4 (7.9) [range: 58, 85]
		128.9 (18.9)
		72.6 (7.4)
			132.2 (16.4)
			70.6 (8.5)

Note. Activity groups do not statistically differ (all p-values>0.25) on any parameters.

Human Physical Activity Measurement

Fitbit Flex2[TM] accelerometers (Fitbit Inc., San Francisco, CA) were used to objectively capture physical activity levels. Participants were instructed to wear the waterproof, triaxial accelerometers on their nondominant wrist during all waking hours. To minimize motivational factors on observational activity data, device feedback was removed (i.e., all informational tiles on phone app deleted and daily "goal" on all devices was set to an unachievable level - 1 million

steps) and participants were instructed to not change app settings. Participants were instructed to sync and charge devices each night. Each Fitbit account was linked to the Fitabase platform (Small Steps Labs, LLC, San Diego, CA), which retrieved data from Fitbit API and aggregated daily step counts. Days with <300 steps were removed for quality control, per published protocols(*132*) and daily steps were averaged over the monitoring period (M = 31.4 days, range: 19-39 days). Participants were dichotomized into "active" versus "sedentary" using average daily step ≥7100, consistent with guidelines for older adults(*133*).

Data and Statistical Analyses

All experiments were randomized and blinded by an independent researcher before plasma or hydrodynamic tail vein injection. Researchers remained blinded throughout histological, biochemical and behavioral assessments. Groups were un-blinded at the end of each experiment upon statistical analysis. Data are expressed as mean ± s.e.m. The distribution of data in each set of experiments was tested for normality using D'Agostino-Pearson omnibus test or Shapiro-Wilk test. Statistical analysis was performed with Prism 8.0 software (GraphPad Software). Means between two groups were compared with two-tailed, unpaired Student's *t*-test. Comparisons of means from multiple groups with each other or against one control group were analyzed with one-way ANOVA followed by appropriate *post hoc* tests (indicated in figure legends). All data generated or analyzed in this study are included in this article.

Exercise Enhances Hippocampal Function Across Ages

Introduction

Exercise increases healthspan in both mice and humans(*68*, *96*, *97*, *101*, *102*). In the aged brain, this manifests as increased adult neurogenesis (*71*, *134*, *135*), and enhancements in hippocampal-dependent learning and memory (*70*, *71*, *136*). Specifically, exercise increases the activation, proliferation, neuronal commitment, and survival of cells along the neurogenic cascade(*70*, *136*, *137*). These enhancements coincide with improved performance in hippocampal-dependent learning and memory tasks, including Morris water maze, fine pattern separation, inhibitory avoidance, object recognition, and contextual fear conditioning tasks(*70*, *99*, *134*, *138*). Similarly, physically active older individuals have increased healthspan, decreased hippocampal atrophy, and more accurate spatial memory recall(*101*, *102*, *139*, *140*). We therefore first evaluated the potential of direct exercise to enhance neurogenesis and cognitive function across ages.

Results

Hippocampal regenerative and cognitive function declines with age

We first characterized the effect of direct exercise on the aged hippocampus. As a control, we assessed age-related cellular and cognitive impairments in the hippocampus of aged (18 months) compared to young (3 months) mice. Using immunohistochemical analysis, we quantified levels of doublecortin (dcx) positive neuroblasts in the young and aged dentate gyrus. Consistent with previous reports demonstrating dramatic declines in neurogenesis with age (*14, 62*), we observed significantly fewer Dcx+ cells in aged mice compared to their young counterparts (**Figure 3.1 A**). We next sought to characterize age-related changes in hippocampal-dependent learning and memory. We used RAWM, Y-maze, and contextual fear conditioning paradigms to evaluate spatial, working, and associative memory, respectively (**Figure 3.1 B-G**). In the training phase of the RAWM paradigm, all mice showed similar spatial learning capacity (**Figure 3.1 C**). However, young animals demonstrated improved learning and memory for the platform location during the testing phase of the task, indicated by fewer errors committed while attempting to find the platform location (**Figure 3.1 B-C**). During the testing phase of Y-Maze, young mice spent significantly more time in the novel arm, compared to the familiar start and trained arms, indicating enhanced spatial working memory (**Figure 3.1 D**). Aged mice, in contrast, spent approximately equal time in all arms. During fear conditioning training, young and aged mice exhibited similar baseline freezing (**Figure 3.1 E**). However, young mice demonstrated increased freezing in contextual (**Figure 3.1 F**), but not cued (**Figure 3.1 G**), memory testing. Altogether, these data establish, that regenerative capacity and hippocampal-dependent cognitive function decline with age in mice.

Exercise increases regenerative and cognitive function in the aged mouse brain

Subsequently, an independent cohort of aged mice was given continuous access to a running wheel for six weeks, while age-matched sedentary control mice were provided with nesting material (**Figure 3.2 A**). After 6 weeks of voluntary exercise, we evaluated effects on neurogenesis using immunohistochemical analysis. While we saw no changes in the number of neural stem cells expressing Sex determining region Y box 2 (Sox2) and Glial fibrillary acidic protein (GFAP), we detected an increase in the number of newly born Dcx-positive neurons in the dentate gyrus of aged exercised compared to aged sedentary mice (**Figure 3.2 B**). We next examined expression of BDNF by Western blot analysis. BDNF is one of the most robust hallmarks of exercise, and is a key modulator of synaptic plasticity and neurogenesis in the hippocampus. We observed increased expression of BDNF in the hippocampus of aged exercised mice compared to their sedentary counterparts (**Figure 3.2 C**). These data indicate that direct exercise stimulates neurogenesis and growth factor expression in the aged hippocampus.

We next tested if direct exercise is sufficient to reverse age-related cognitive impairments using RAWM and fear conditioning behavioral paradigms. In both the training and testing phases of RAWM, aged exercised mice demonstrated enhanced spatial learning and memory capacity compared to their sedentary counterparts (**Figure 3.2 D-E**). During fear conditioning training, aged exercised and sedentary mice exhibited similar baseline freezing (**Figure 3.2 F**). However, aged exercised mice demonstrated increased freezing in contextual (**Figure 3.2 G**), but not cued (**Figure 3.2 H**), memory testing. These data indicate that exercise is sufficient to enhance spatial and associative learning and memory in aged mice.

Exercise increases regenerative and cognitive function in the mature mouse brain

Exercise has been shown to function across ages, enhancing regenerative and cognitive capacity in young and aged animals(*71*). Thus, we also examined the potential of direct exercise to enhance hippocampal function in mice at younger ages. Mature (6-7 month) mice were given continuous access to a running wheel for six weeks, while age-matched sedentary control mice were provided with nesting material (**Figure 3.3 A**). After 6 weeks, we evaluated effects on neurogenesis, BDNF, and cognition in line with our assessment of aged exercised mice. Mature exercised mice demonstrated an increase in the number of newly born Dcx-positive neurons (**Figure 3.3 B**) and higher expression of hippocampal BDNF (**Figure 3.3 C**) when compared to their sedentary counterparts. We next assessed spatial learning and memory using RAWM. During the training phase, mature exercised and sedentary mice demonstrated similar capacity to learn the task (**Figure 3.3 D**). However, mature exercised mice committed fewer errors while attempting to find the platform on the testing day, indicating improved spatial memory recall (**Figure 3.3 D-E**). Finally, while no differences were observed in baseline freezing during fear conditioning training (**Figure 3.3 F**), mature exercised mice demonstrated increased freezing in contextual memory testing (**Figure 3.3 G**). Similar to aged exercised and sedentary mice, mature exercised mice performed equivalent to their sedentary counterparts in cued fear conditioning (**Figure 3.3 H**). Altogether, these data demonstrate that exercise enhances cellular and cognitive function in the hippocampus across ages.
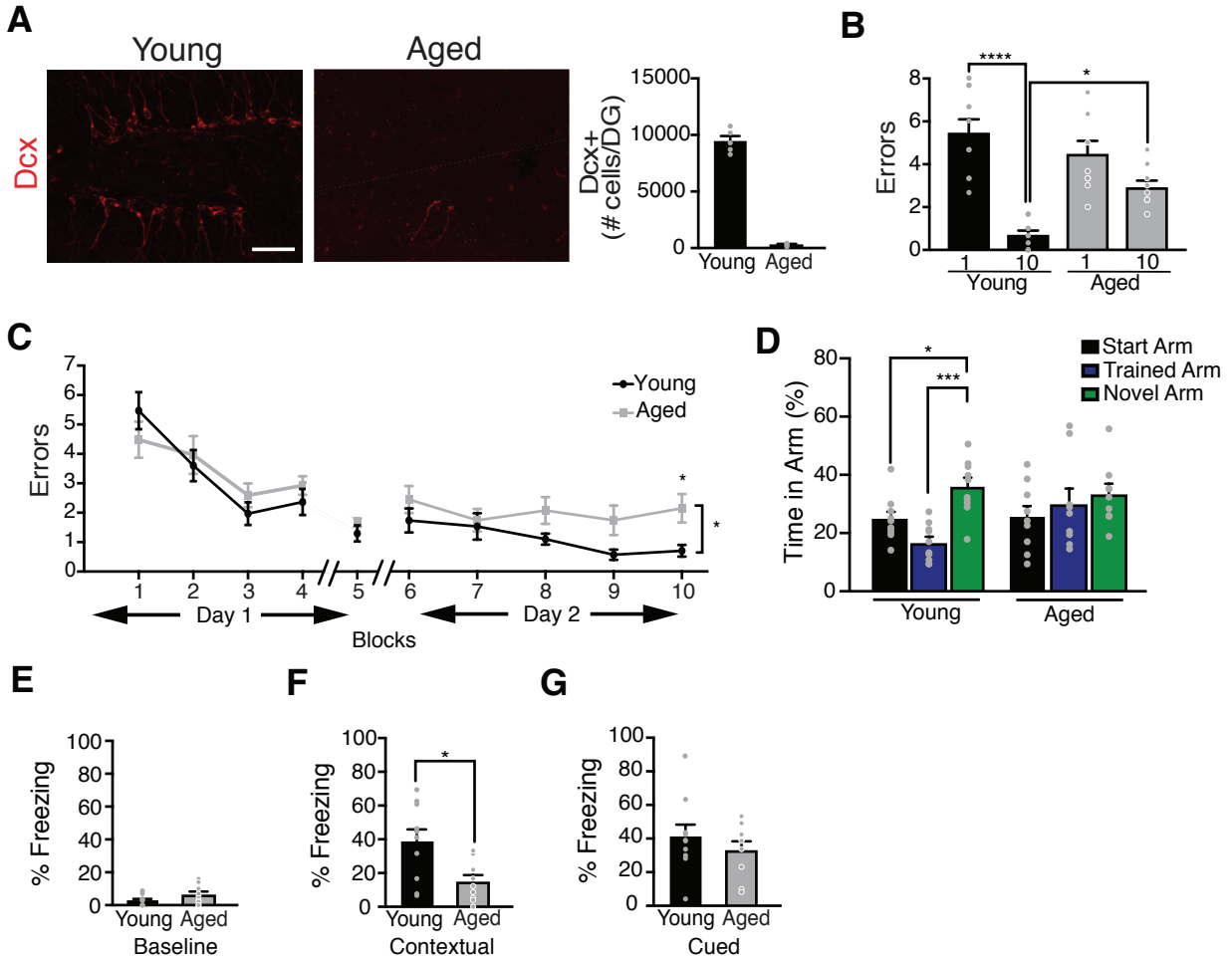
Figure 3.1. Characterization of age-related hippocampal cellular and cognitive impairments. (**A**) Representative field and quantification of Dcx-positive cells in the DG of the hippocampus of young (5 months) and aged (18-20 months) mice (n=5 per group; Arrowheads point to individual cells; scale bar 100 μm). (**B,C**) Spatial learning and memory were assessed by radial arm water maze (RAWM) as number of entry errors committed during the training and testing phases. Overall learning and memory was analyzed between Block 1 and 10 (1 Block = 3 Trials; n=9-10 per group). (**D**) Spatial working memory was assessed by Y-Maze as time spent in the start, trained, and novel arms during the testing phase (n=10 per group). (**E-G**) Associative fear memory was assessed using contextual (**F**) and cued (**G**) fear conditioning as percent time spent freezing 24 hours after training (n=10 per group). Baseline freezing (**E**) was assessed as time spent freezing prior to fear conditioning. All data are shown as mean±s.e.m.; *P<0.05, ***P<0.001, ****P<0.0001, *t* test (**A,E,F,G**); repeated measures analysis of variance (ANOVA) with Bonferroni post-hoc test (**C**); ANOVA with Tukey's post-hoc test (**B,D**).
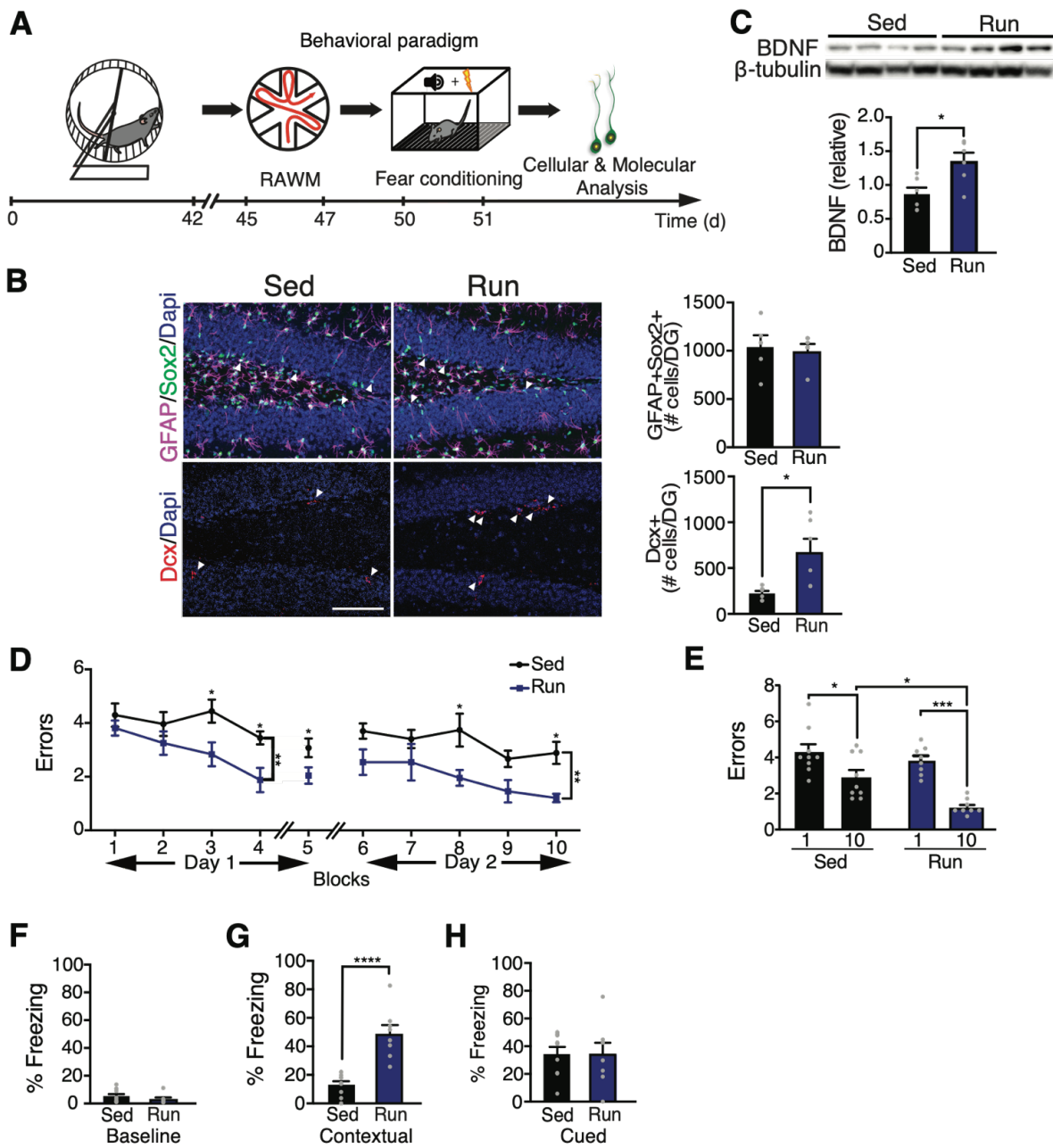
Figure 3.2. Exercise benefits the aged hippocampus at the cellular and cognitive level.
(**A**) Aged (18 months) mice were given voluntary access to a running wheel for 6 weeks (exercise) or maintained as sedentary controls. Schematic illustrates chronological order used for exercise, cognitive testing, and cellular and molecular analysis. (**B**) Representative microscopic fields and quantification of GFAP/Sox2 double-positive and Dcx-positive cells in the dentate gyrus (DG) of the hippocampus of aged exercise and sedentary mice (n=5-9 per group; Arrowheads point to individual cells; scale bar 100µm). (**C**) Western blot and quantification of BDNF in the hippocampus of aged exercise and sedentary mice (n=7 per group). Quantification normalized to β-Tubulin. (**D,E**) Spatial learning and memory were assessed by radial arm water maze (RAWM) as number of entry errors committed during the training and testing phases. Overall learning and memory was analyzed between Block 1 and 10 (n=8-9 per group). (**F-H**) Associative fear memory was assessed using contextual (**G**) and cued (**H**) fear conditioning as percent time spent freezing 24 hours after training. Baseline freezing (**F**) was assessed as time spent freezing prior to fear conditioning (n=8-9 per group). All data are shown as mean±s.e.m.; *P<0.05, ***P<0.001, ****P<0.0001, *t* test (**B,C,F-H**)**;** repeated measures analysis of variance (ANOVA) with Bonferroni post-hoc test (**D**); ANOVA with Tukey's post-hoc test (**E**).
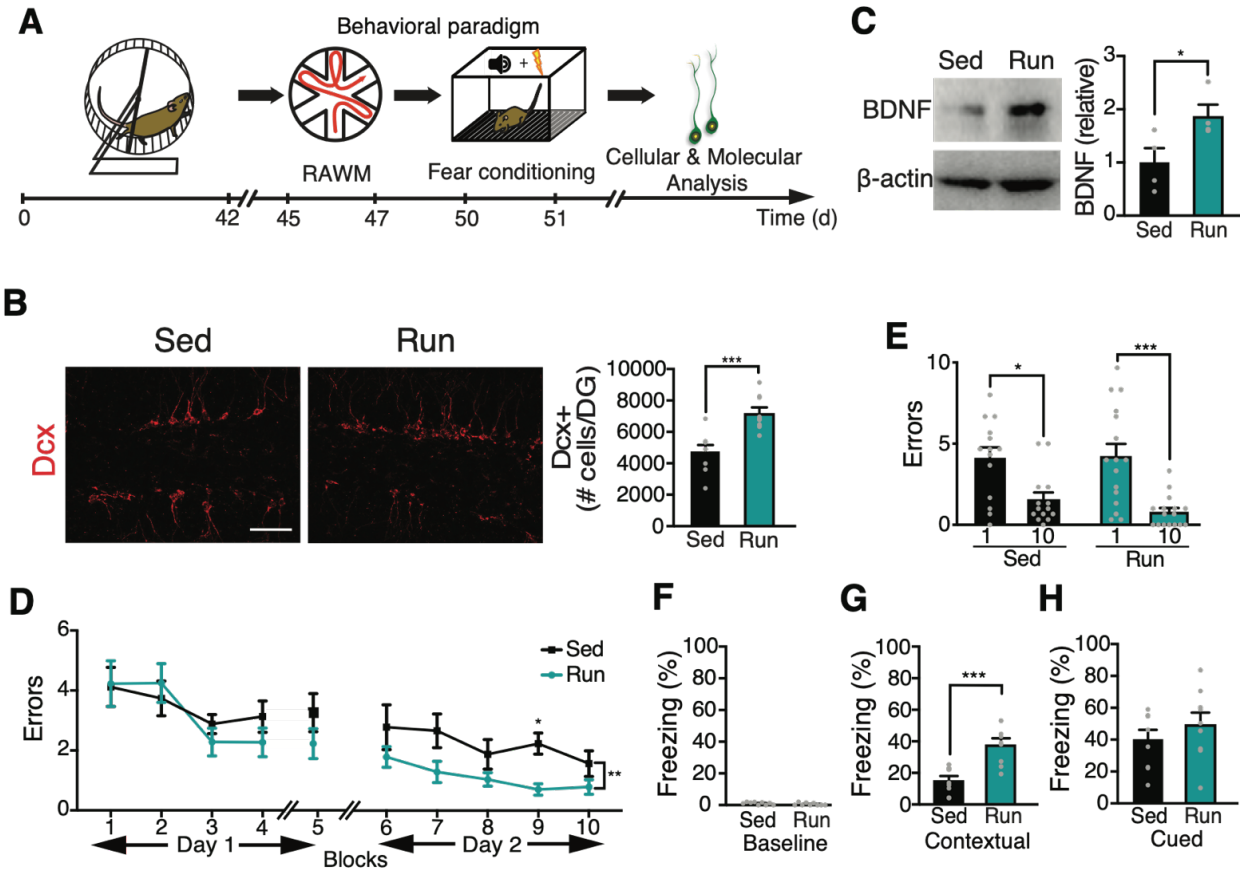
Figure 3.3. Exercise enhances cellular and cognitive function in the mature hippocampus. (**A**) Mature (6-7 months) mice were given voluntary access to a running wheel for 6 weeks (exercise) or maintained as sedentary controls. Schematic illustrates chronological order used for exercise, cognitive testing, and cellular and molecular analysis. (**B**) Representative microscopic fields and quantification of Dcx-positive cells in the dentate gyrus of the hippocampus of mature exercise and sedentary mice (n=9 per group; scale bar 100⎡m). (**C**) Western blot and quantification of BDNF in the hippocampus of mature exercise and sedentary mice (n=4 per group). Quantification normalized to ®-Actin. (**D,E**) Spatial learning and memory were assessed by radial arm water maze (RAWM) as number of entry errors committed during the training and testing phases. Overall learning and memory was analyzed between Block 1 and 10 (n=14-16 per group). (**F-H**) Associative fear memory was assessed using contextual (**G**) and cued (**H**) fear conditioning as percent time spent freezing 24 hours after training (n=9 per group). Baseline freezing (**F**) was assessed as percent time spent freezing prior to fear conditioning (n=9 per group). All data are shown as mean±s.e.m.; *P<0.05, **P<0.01, ***P<0.001, *t* test (**B,C,F-H**); repeated measures analysis of variance (ANOVA) with Bonferroni post-hoc test (**D**); ANOVA with Tukey's post-hoc test (**E**).

Blood Factors Transfer Benefits of Exercise on Neurogenesis and Cognition to the Aged Brain

Introduction

Despite the evident benefit of exercise on the aged brain, little data exists to explain how exercise exerts these rejuvenating effects(*141*). To date, some potential mechanisms, such as elevated growth factor levels or muscle-derived factors, have been proposed to explain the regenerative and cognitive benefit of exercise(*112*, *113*, *115*, *122*). These data posit exercise as a systemic modulator of brain function. In parallel, a growing field of aging biology based on the model of heterochronic parabiosis has likewise begun to demonstrate the potential of systemic manipulations to rejuvenate the aged brain(*62*, *69*). Like exercise, exposure to a young circulation through heterochronic parabiosis or young blood plasma administration reverses age-related impairments in hippocampal regenerative and cognitive function(*19*). The rejuvenating effects observed with exercise mirror those of young blood exposure, raising the possibility that exercise similarly functions through blood factors to exert its beneficial effects. We therefore hypothesized that exercise-induced circulating blood factors mediate the rejuvenating effects of exercise on regenerative and cognitive function in the aged brain.

Results

Systemic blood plasma administration transfers the benefits of exercise on neurogenesis to the aged brain.

We tested whether the benefits of exercise on the aged hippocampus could be transferred through administration of exercise-induced circulating blood factors. After 6 weeks of voluntary exercise, blood was collected and plasma was isolated from exercised and sedentary aged mice and pooled by group. An independent cohort of naïve aged mice was then intravenously injected with plasma from exercised or sedentary aged mice eight times over three weeks (**Figure 4.1 A**). We analyzed adult neurogenesis by immunohistochemical analysis. Although no difference in the number of neural stem cells expressing Sox2 and GFAP was observed (**Figure 4.1 B**), we detected an increase in the number of newly born neurons containing Dcx in the dentate gyrus region of the hippocampus in aged animals administered plasma from exercised mice (**Figure 4.1 B**). We assessed neuronal differentiation and survival by BrdU incorporation. Mature differentiated neurons express both BrdU and the neuronal marker NeuN. Aged mice administered with plasma from exercised mice showed an increase in the number of mature neurons expressing both BrdU and NeuN in the dentate gyrus (**Figure 4.1 B**). We examined expression of BDNF by Western blot and observed an increase in hippocampal expression in animals administered plasma from exercised mice (**Figure 4.1 C**). Together, these data indicate that systemic administration with plasma from exercised aged animals can transfer the beneficial effect of exercise on regenerative capacity in the aged hippocampus.

Systemic blood plasma administration transfers the benefits of exercise on cognition to the aged brain.

To assess the potential of plasma from exercised mice to rescue age-related impairments in hippocampal-dependent learning and memory, we used RAWM and contextual fear conditioning paradigms (**Figure 4.1 A**). In the training phase of the RAWM paradigm all mice showed similar spatial learning capacity (**Figure 4.1 D**). Aged animals administered plasma from aged mice that exercised demonstrated improved learning and memory for the platform location during the testing phase of the task compared to that of animals treated with plasma from sedentary aged mice (**Figure 4.1 D-E**). During fear conditioning training, all mice exhibited similar baseline freezing regardless of treatment (**Figure 4.1 F**). However, aged mice receiving plasma from exercised aged mice demonstrated increased freezing in contextual (**Figure 4.1 G**), but not cued (**Figure 4.1 H**) memory testing. These data indicate that exercise-induced circulating blood factors in plasma can ameliorate impairments in hippocampal-dependent learning and memory in aged mice.

Systemic blood plasma administration transfers the benefits of exercise across ages.

Exercise enhances regenerative capacity in young(*137*, *142*, *143*) and aged(*37*, *70*, *99*, *134*) animals. Correspondingly, we investigated whether the beneficial effects of exercise observed in mice at younger ages could also be transferred to aged mice through circulating blood factors. We administered plasma derived from exercised or sedentary mature (6-7 months) mice to aged mice. As a control, we examined the effect of direct exercise on the hippocampus of mature mice (**Figure 3.3**). Exercise promoted neurogenic and cognitive enhancements in the hippocampus of mature mice (**Figure 3.3 C-H**). After, we collected blood and isolated plasma from exercised and sedentary mature mice and pooled the plasma by group. Naïve aged mice

were intravenously injected with the plasma (**Figure 4.2 A**). Previous work has demonstrated that young blood plasma from sedentary mice is sufficient to rejuvenate the aged brain(*62*); however, it is unknown at what ages the effect of young blood wanes. Therefore, to account for any potential residual young blood benefit that persists at mature ages, an additional aged control group was administered saline. No significant changes were observed between aged mice administered plasma from sedentary mature mice or saline. However, administration of plasma from exercised mature mice resulted in increased adult neurogenesis compared to controls (**Figure 4.2 B**). Thus, exercise-induced circulating blood factors across ages can confer the benefits of exercise on the aged hippocampus.
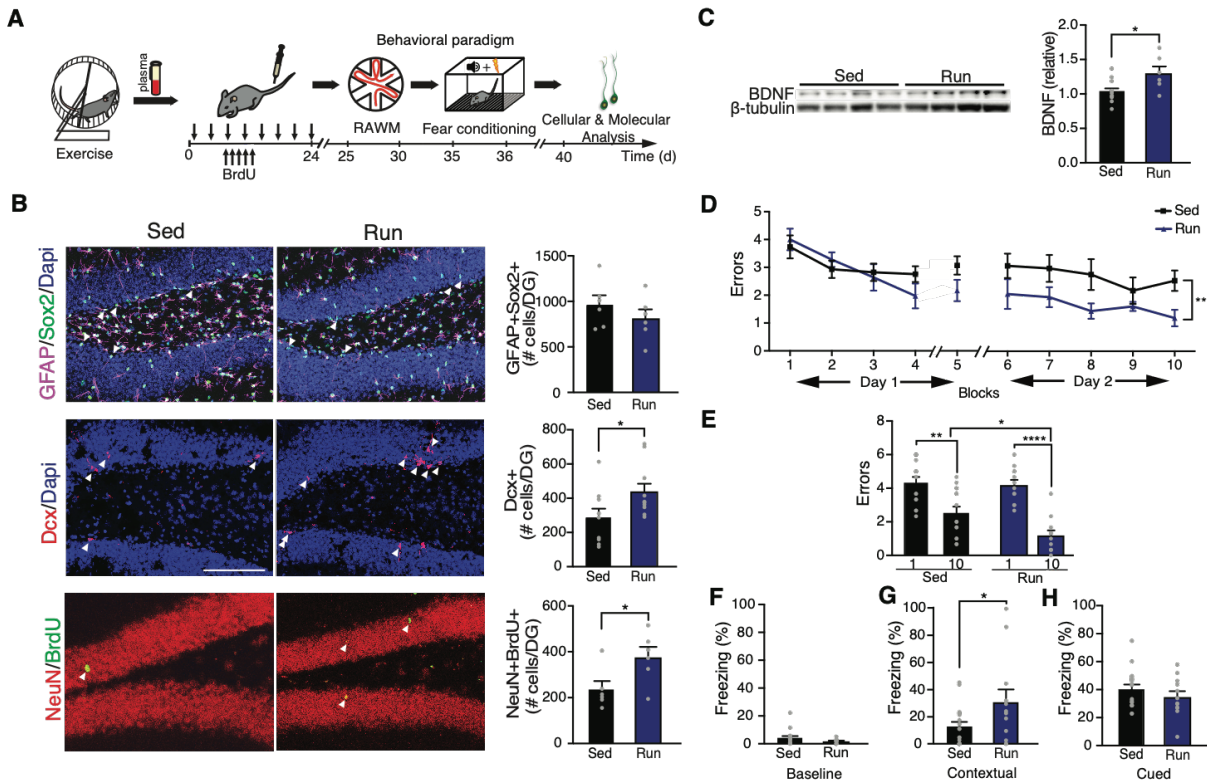
Figure 4.1. Systemic administration of exercise-induced circulatory blood factors ameliorates impaired neurogenesis and cognition in the aged hippocampus. (**A**) Plasma was collected from aged (18 months) exercised or sedentary mice and administered to sedentary aged mice 8 times over 24 days (100ul per intravenous injection). Schematic illustrates chronological order of plasma administration from exercised aged mice and cognitive testing. (**B**) Representative microscopic fields and quantification of GFAP/Sox2 double-positive, Dcx-positive, and NeuN/BrdU double-positive cells in the DG of the hippocampus of naïve aged mice administered aged exercise or sedentary plasma (n=10-11 per group; Arrowheads point to individual cells; scale bar 100μm). (**C**) Western blot and quantification of BDNF in the hippocampus of naïve aged mice administered aged exercise or sedentary plasma (n=6-10 per group). Quantification normalized to β-Tubulin. (**D,E**) Spatial learning and memory were assessed by radial arm water maze (RAWM) as number of entry errors committed during the training and testing phases. Overall learning and memory was analyzed between Block 1 and 10. (1 Block = 3 Trials; n=12-15 per group). (**F-H**) Associative fear memory was assessed using contextual (**G**) and cued (**H**) fear conditioning as percent time spent freezing 24 hours after training. Baseline freezing (**F**) was assessed as percent time spent freezing prior to fear conditioning (n=12-19 per group). All data are shown as mean±s.e.m.; *P<0.05, **P<0.01, ****P<0.0001 *t* test (**B,C,F-H**); repeated measures analysis of variance (ANOVA) with Bonferroni post-hoc test (**D**); ANOVA with Tukey's post-hoc test (**E**).
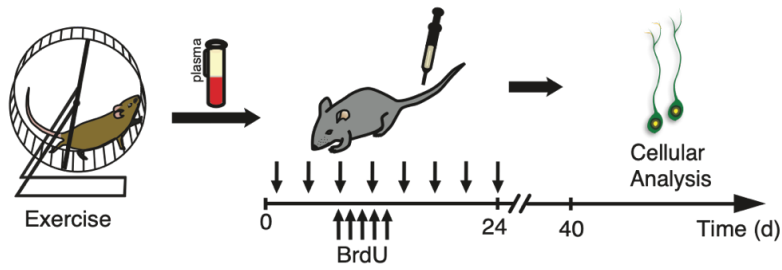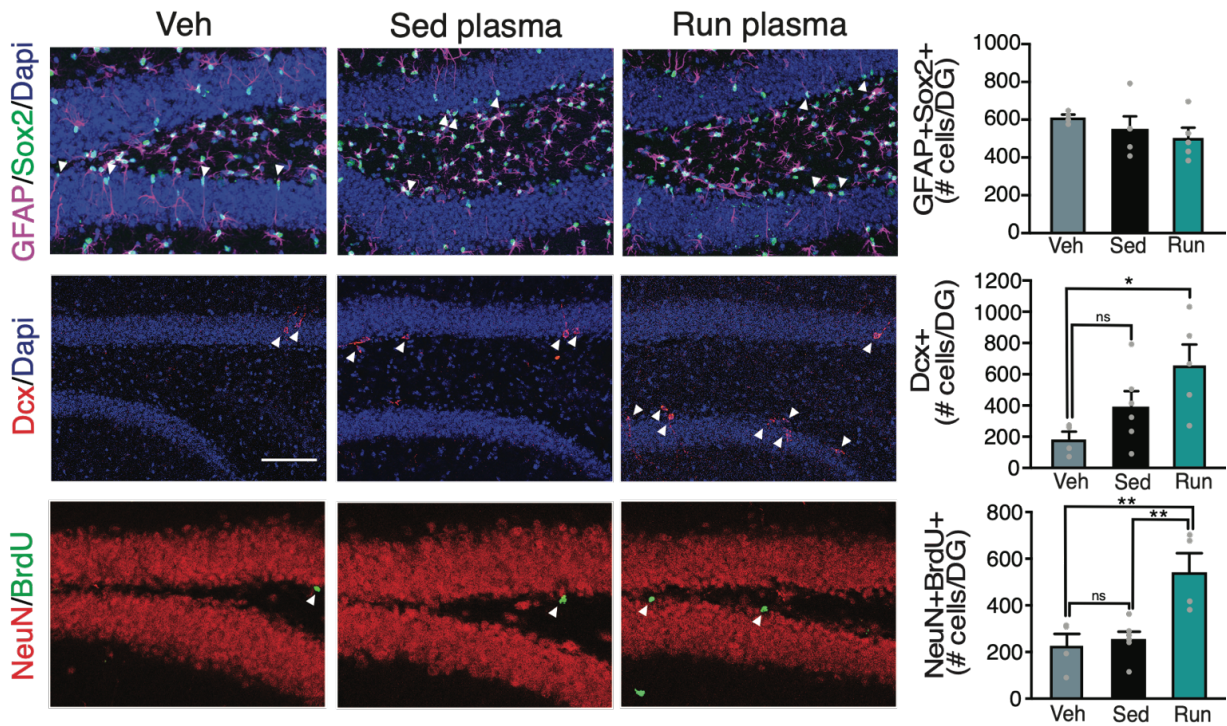
Figure 4.2. Systemic administration of exercise-induced circulating factors in mature blood increases adult hippocampal neurogenesis in aged mice. (**A**) Blood plasma was collected from mature (7 months) exercised or sedentary mice and administered to sedentary aged mice 8 times over 24 days (100ul per intravenous injection). Schematic illustrates chronological order of mature exercise plasma administration and cellular analysis. (**B**) Representative microscopic fields and quantification of GFAP/Sox2 double-positive, Dcx-positive, and NeuN/BrdU double-positive cells in the DG of the hippocampus of naïve aged mice administered mature exercise or sedentary plasma (n=4-6 per group; arrowheads point to individual cells; scale bar 100μm). All data are shown as mean±s.e.m.; *P<0.05, **P<0.01; ANOVA with Tukey's post-hoc test (**B**).

GPLD1 Ameliorates Age-Related Regenerative and Cognitive Decline in Mice

Introduction

Given that plasma from both exercised aged and mature mice alleviated age-related impairments in the hippocampus, we sought to identify individual circulating blood factors mediating these effects. It is critical to identify individual factors to develop accessible approaches by which the benefits of exercise may be therapeutically transferred. Individual pro-aging(*20*, *88*, *89*, *91*, *144*) or pro-youthful(*69*, *94*) blood factors have previously been identified that can, to an extent, recapitulate the benefits of heterochronic parabiosis or young blood plasma exposure. Similarly, multiple factors have been implicated in the effects of exercise(*111*, *113*, *115*, *119*, *122*). However, evidence is limited that these factors are sufficient to mimic the effects of exercise, and their roles have yet to be tested in the context of normal aging. We hypothesized that individual, exercise-induced circulating blood factors would be sufficient to mimic the benefits of exercise on regenerative and cognitive function in the aged brain.

Results

Gpld1 is an exercise-induced, liver-derived circulating blood factor

We used isobaric tagging together with liquid chromatography tandem mass spectrometry to measure relative amounts of soluble proteins in the plasma from exercised or sedentary aged and mature mice. Abundance of 30 factors increased after exercise in aged mice (**Figure 5.1 A, Figure 5.2A**), and 33 factors increased after exercise in mature mice (**Figure 5.1 A, Figure 5.2 B**). According to the Tabula Muris compendium of single cell transcriptome data from mice(*145*) and the protein atlas(*146*), 63% and 67% of exercise-induced factors in aged and mature mice respectively, are predominantly expressed in the liver. Abundance of 12 factors – Gpld1, Cholinesterase (Bche), Napsin A (Napsa), Serum paraoxonase 1 (Pon1), Glutathione peroxidase 3 (Gpx3), Mannose binding protein C (Mbl2), Inhibitor of carbonic anhydrase (Ica), Inter-alpha-trypsin inhibitor heavy chain H2 (Itih2), Phospholipid transfer protein (Pltp), Carbonic anhydrase 2 (Ca2), Alpha-1-antitrypsin 1-1 (Serpina1a) and Alpha-1-antitrypsin 1-4 (Serpina1d) – was increased in plasma from exercised aged and mature animals (**Figure 5.1 A**). Functional enrichment analysis of these factors using search tool for the retrieval of interacting genes/proteins (STRING) identified largely metabolic processes, in which Gpld1 and Pon1 were overrepresented (**Figure 5.1 B**). We elected to investigate Gpld1, a glycosylphosphatidylinositol (GPI) degrading enzyme(*147*) not previously linked to aging, neurogenesis or cognition.

Amounts of Gpld1 were confirmed to increase in plasma of individual aged (**Figure 5.1 C**) and mature (**Figure 5.1 D**) exercised mice compared to those in plasma from sedentary age-matched controls. In exercised and sedentary aged mice, we observed a significant correlation between increased Gpld1 concentrations in plasma and improved cognitive performance in the RAWM and contextual fear conditioning behavioral tests (**Figure 5.1 E-F**). Furthermore, we detected an increase in Gpld1 in plasma from active compared to sedentary healthy elderly human individuals (**Figure 5.1 G**). These data identify Gpld1 as an exercise-induced circulating

blood factor in aged mice and humans with potential relevance to cognitive function in mice.

To identify the potential source of exercise-induced systemic Gpld1, we characterized Gpld1 mRNA expression in mouse liver, lung, fat, spleen, skin, kidney, heart, muscle, cortex, hippocampus and cerebellum (**Figure 5.3 A**). We detected highest Gpld1 expression in the liver (**Figure 5.3 A**), consistent with previous reports identifying the liver as the primary source of circulating Gpld1(*148*). We examined whether Gpld1 mRNA expression changed in the liver as a function of aging, exercise, or plasma administration. No changes in Gpld1 expression were detected during aging or following plasma administration (**Figure 5.4 A-B**). Gpld1 expression was increased in the liver of exercised aged mice compared to that in sedentary animals (**Figure 5.3 B**). As a control, we evaluated Gpld1 expression in muscle and hippocampus and observed no changes under any condition (**Figure 5.4 C-I**). We also observed no change in circulating levels of Gpld1 in plasma with age (**Figure 5.4 J**). These data are consistent with a role of Gpld1 as a liver-derived exercise-induced circulating factor in aged mice.

Selectively increasing systemic Gpld1 enhances neurogenesis and cognition in the aged brain

To test the effect of Gpld1 on the aged hippocampus, we used hydrodynamic tail vein injection (HDTVI)-mediated *in vivo* transfection to overexpress Gpld1 in the liver. Aged mice were injected with expression constructs encoding either Gpld1 or green fluorescent protein (GFP) control, and analysis was done in a timeframe consistent with our previous plasma administration experiments (**Figure 5.3 C**). Increased Gpld1 mRNA expression in the liver and increased Gpld1 plasma concentrations were confirmed after HDTVI in aged mice (**Figure 5.3 D-E**). By immunohistochemistry and Western blot analysis, we detected an increase in adult neurogenesis (**Figure 5.3 F**) and expression of BDNF (**Figure 5.3 G**) in the hippocampus of aged mice overexpressing Gpld1 in liver. To assess the effect of Gpld1 overexpression on hippocampal-

dependent learning and memory, we used RAWM, forced alteration Y maze and novel object recognition tests (**Figure 5.3 C**). Aged animals overexpressing Gpld1 committed significantly fewer errors in locating the target platform during the RAWM training and testing phases (**Figure 5.3 H-I**) compared to controls. During Y maze and novel object recognition testing, aged mice overexpressing Gpld1 spent significantly more time in the novel arm (**Figure 5.3 J**) and with the novel object (**Figure 5.3 K**). We also tested whether increasing Pon1, the second liver-derived circulating factor overrepresented in our exercise proteomic functional enrichment analysis (**Figure 5.1 B**), ameliorated age-related impairments in hippocampal-dependent cognitive function. Aged mice were given HDTVI with expression constructs encoding either Pon1 or GFP control (**Figure 5.5 A-B**); however, no cognitive improvements were observed in a timeframe consistent with Gpld1 experiments (**Figure 5.5 C-F**). Together, these data indicate that selectively increasing liver-derived systemic concentrations of Gpld1 is sufficient to improve adult neurogenesis and cognitive function in the aged hippocampus.

A

Aged

18

vs.

12

21

vs.

Mature

Gpld1
Bche
Napsa
Pon1
Gpx3
Mbl2
Ica
Itih2
Pltp
Ca2
Serpina1a
Serpina1d

B

Biological Processes

Positive regulation of transport — Gpld1, Pon1 — 5
Organic hydroxy compound metabolic process — Gpld1, Pon1 — 4
Ammonium ion metabolic process — Gpld1, Pon1 — 3
Positive regulation of cholesterol efflux — Pon1 — 2
Response to hormone — Gpld1 — 5
Ethanolamine-containing compound metabolic process — Gpld1, Pon1 — 3

-log2(FDR)

C

Aged Mouse

Sed   Run

Gpld1

Ponceau

Plasma Gpld1 (relative)

*

Sed   Run

D

Mature Mouse

Sed   Run

Gpld1

Ponceau

Plasma Gpld1 (relative)

*

Sed   Run

E

Errors (Block 10)

Gpld1

p = 0.0074
R^2 = 0.7239

● Run
● Sed

F

% Freezing

Gpld1

p = 0.0046
R^2 = 0.7628

G

Elderly Human

Sed   Active

Gpld1

Ponceau

Plasma Gpld1 (relative)

*

Sed   Active

44

Figure 5.1. Exercise increases systemic levels of Gpld1 in mature and aged mice and healthy elderly humans. (**A**) Venn diagram of results from aged exercise and mature exercise proteomic screens. In blue are the number of proteins that increase with exercise in aged (18 months) mice, and in teal are proteins that increase with exercise in mature (7 months) mice. Listed are the 12 proteins that increase with exercise in both aged and mature mice. (**B**) Enrichment analysis of 12 proteins upregulated by exercise in mature and aged mice. Gpld1 and Pon1 are listed next to the processes in which they are implicated. The number of proteins represented in each process is listed to the right of the bar. (**C,D**) Western blots with corresponding Ponceau S stains and quantification of Gpld1 in equal volumes of blood plasma from individual aged (**C**) and mature (**D**) exercise and sedentary mice (n=4-5 per group). (**E,F**) Correlation between plasma Gpld1 levels in aged exercise and sedentary mice and number of errors committed during the final block of RAWM (**E**) or time spent freezing in contextual fear conditioning (**F**). (**G**) Western blot and quantification of Gpld1 in equal volumes of blood plasma from individual active (>7100 steps per day) and sedentary (<7100 steps per day) healthy elderly (66-78 years) humans (n=8-12 per group). All data are shown as mean±s.e.m.; *P<0.05, *t* test (**C,D,G**), linear regression (**E,F**).

A

Aged Up

Flt4	Hbb-b1
Apoa1	Mug1
Afm	Man1a1
Il1rap	Lum
Gsn	Ttr
Ldha	C8g
Lifr	Serpina3m
Cfd	Fcn1
Cpn2	Dmd
Gpld1	Gpx3
Bche	Mbl2
Napsa	Ica
Pon1	Itih2
Pltp	Serpina1a
Ca2	Serpina1d

B

Mature Up

C8a	Serpina10
Serpina1e	Mbl1
Itih1	Apoc1
Vtn	Fbln1
H2-Q10	Krt42
C8b	Itih3
Cfp	Blvrb
Serpina3k	Hrg
Cd5l	Svs6
C1ra	Serpina1b
Cpn1	Gpx3
Gpld1	Mbl2
Bche	Ica
Napsa	Itih2
Pon1	Serpina1a
Pltp	Serpina1d
Ca2	

Figure 5.2. Proteomic analysis of exercise-induced circulating blood factors in mature and aged mice.
(**A**) List of 30 proteins upregulated in blood plasma of aged mice with exercise. (**B**) List of 33 proteins upregulated in blood plasma of mature mice with exercise.

Figure 5.3. Increased systemic GPLD1 ameliorates impaired neurogenesis and cognition in the aged hippocampus. (**A,B**) Quantitative reverse-transcriptio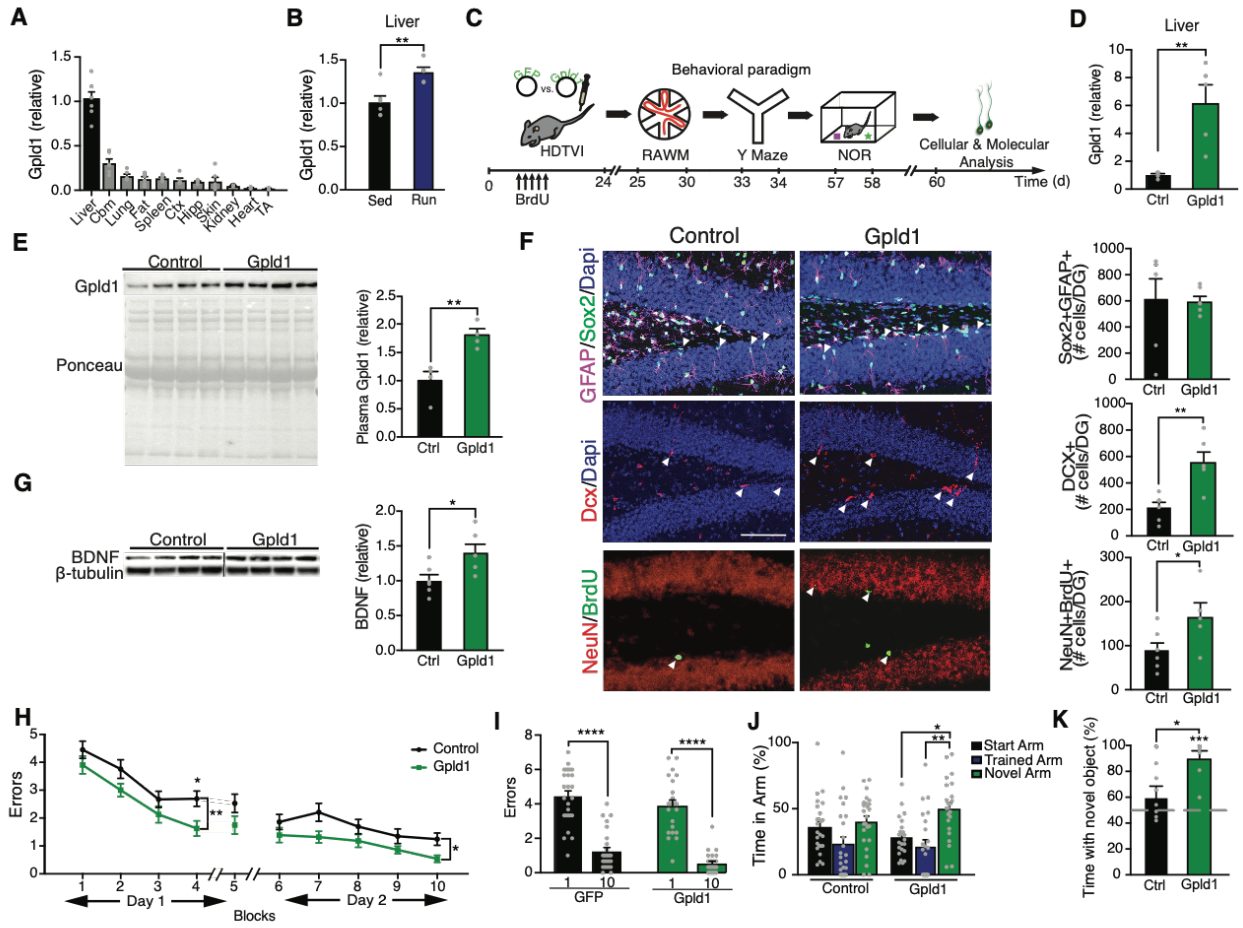n PCR of Gpld1 across tissues in sedentary mice (**A**), and in liver of aged exercised and sedentary mice (**B**). Gene expression relative to Gapdh (n=5-6 per group). Abbreviations: Cbm, cerebellum; Ctx, cortex; Hipp, hippocampus; TA, tibialis anterior muscle. (**C**) Aged (18 months) mice were given hydrodynamic tail vein injections (HDTVI) of expression constructs encoding either Gpld1 or GFP control. Schematic illustrates chronological order of HDTVI, cognitive testing, and cellular and molecular analysis. (**D**) Quantitative reverse-transcription PCR of Gpld1 in liver of aged mice expressing Gpld1 or GFP control. Gene expression relative to Gapdh (n=5 per group). (**E**) Western blot with corresponding Ponceau S stain and quantification of Gpld1 in equal volumes of blood plasma from individual aged mice expressing Gpld1 or GFP control (n=4 per group). (**F**) Representative microscopic fields and quantification of GFAP/Sox2 double-positive, Dcx-positive, and NeuN/BrdU double-positive cells in the DG of the hippocampus of aged mice expressing Gpld1 or GFP control (n=6 per group; Arrowheads point to individual cells; scale bar 100μm). (**G**) Western blot and quantification of BDNF in the hippocampus of aged mice expressing Gpld1 or GFP control (n=6 per group). Quantification normalized to β-Tubulin. (**H,I**) Spatial learning and memory were assessed by radial arm water maze (RAWM) as number of entry errors committed during the training and testing phases. Overall learning and memory was analyzed between Block 1 and 10 (1 Block = 3 Trials; n=26 per group). (**J**) Spatial working memory was assessed by Y-Maze as time spent in the start, trained, and novel arms during the testing phase (n=23-25 per group). (**K**) Object recognition memory was assessed by Novel Object Recognition (NOR) as time spent exploring a novel object 24 hours after training (n=8-12 per group). All data are shown as mean±s.e.m.; *P<0.05, **P<0.01, ***P<0.001, ****P<0.0001; *t* test (**B,D,E-G,K**); repeated measures analysis of variance (ANOVA) with Bonferroni post-hoc test (**H**); ANOVA with Tukey's post-hoc test (**I,J**); One-sample *t* test versus 50% (**K**).
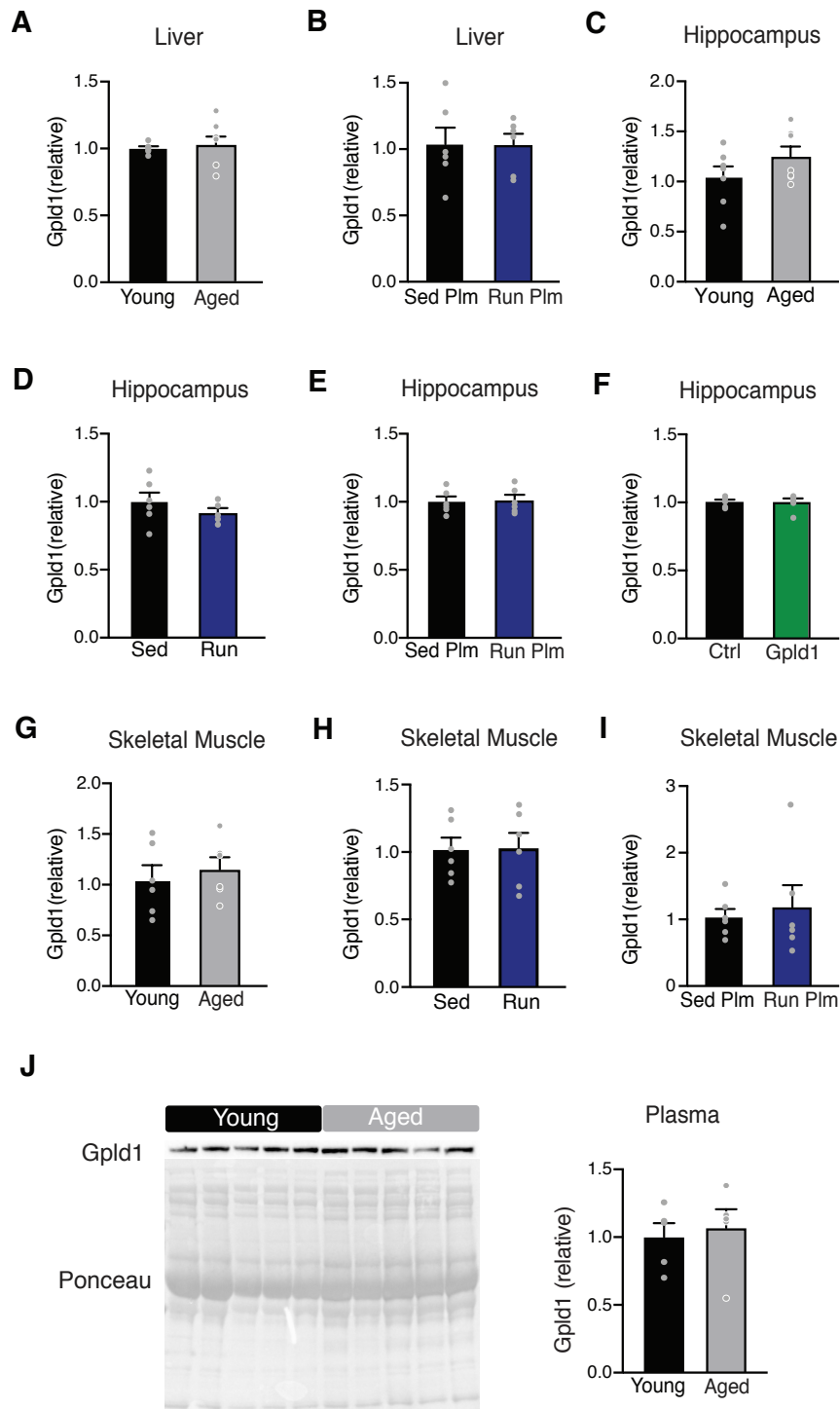
Figure 5.4. Characterization of Gpld1 expression with aging, exercise, aged exercise plasma administration, and Gpld1 HDTVI. (**A-I**) Quantitative reverse-transcription PCR of Gpld1 in: liver of young and aged sedentary mice (**A**), liver of aged mice administered aged exercise or sedentary plasma (**B**), hippocampus of young and aged sedentary mice (**C**), hippocampus of aged exercised and sedentary mice (**D**), hippocampus of aged mice administered aged exercise or sedentary plasma (**E**), hippocampus of Gpld1 HDTVI mice (**F**), skeletal muscle of young and aged sedentary mice (**G**), skeletal muscle of aged exercised and sedentary mice (**H**), and skeletal muscle of aged mice administered aged exercise or sedentary plasma (**I**). Gene expression relative to Gapdh (n=5-6 per group). (**J**) Western blot with corresponding Ponceau S stain and quantification of Gpld1 in equal volumes of blood plasma from individual young or aged mice (n=5 per group). All data are shown as mean±s.e.m.; *t* test (**A-J**).
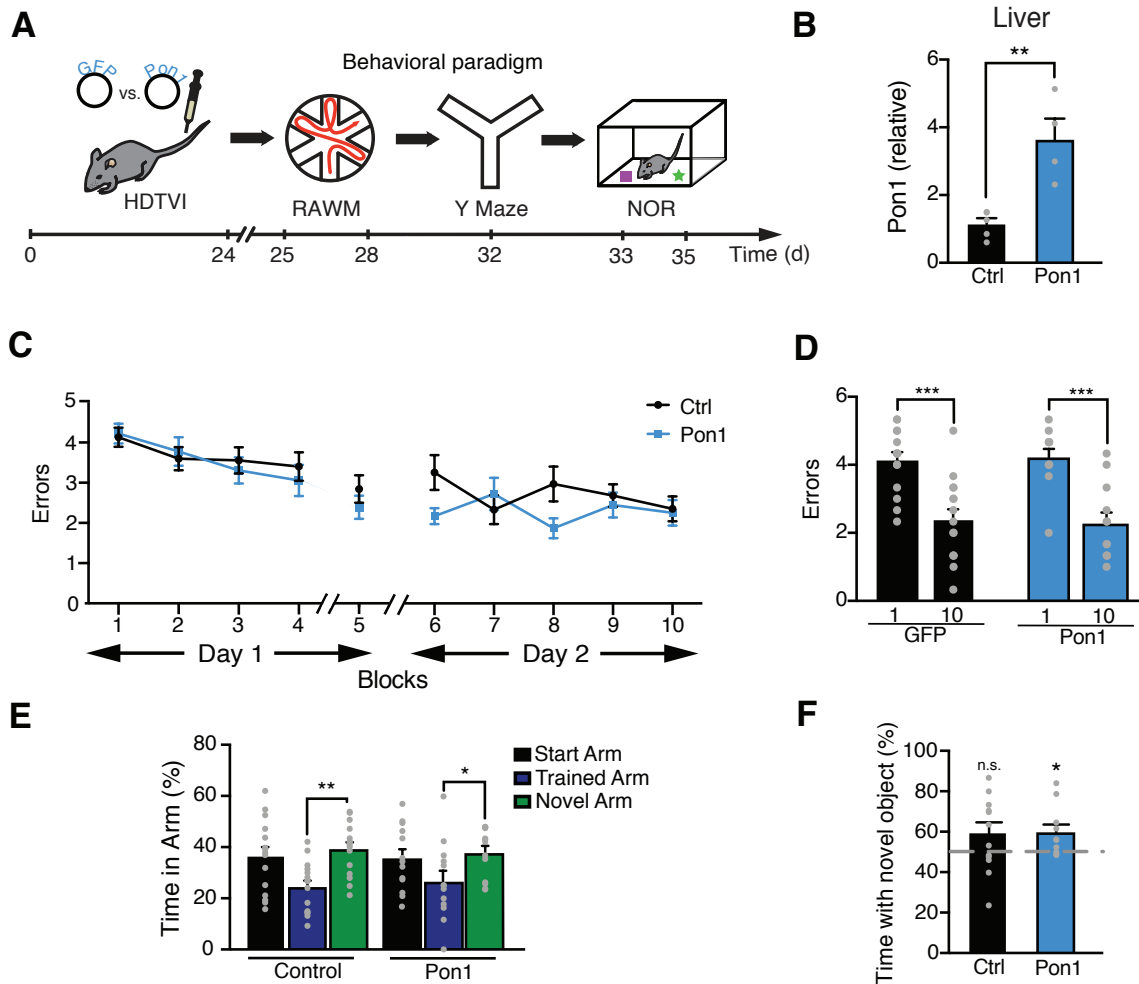
Figure 5.5. Increased systemic Pon1 does not improve cognition in the aged hippocampus. (**A**) Aged (22 months) mice were given hydrodynamic tail vein injections (HDTVI) of expression constructs encoding either Pon1 or GFP control. Schematic illustrates chronological order of HDTVI and cognitive testing. (**B**) Quantitative reverse-transcription PCR of Pon1 in liver of GFP and Pon1 HDTVI mice. Gene expression relative to Gapdh (n=5 per group). (**C-D**) Spatial learning and memory were assessed by radial arm water maze (RAWM) as number of entry errors committed during the training and testing phases. Overall learning and memory was analyzed between Block 1 and 10 (n=12-15 per group). (**E**) Spatial working memory was assessed by Y-Maze as time spent in the start, trained, and novel arms during the testing phase (n=13-15 per group). (**F**) Object recognition memory was assessed by Novel Object Recognition (NOR) as time spent exploring a novel object 24 hours after training (n=11-12 per group). All data are shown as mean±s.e.m.; *P<0.05, **P<0.01, ***P<0.001; *t* test (**B**); repeated measures analysis of variance (ANOVA) with Bonferroni post-hoc test (**C**); ANOVA with Tukey's post-hoc test (**D,E**); One-sample *t* test versus 50% (**F**).

GPI-anchored substrate cleavage is necessary for the effects of Gpld1 on the aged hippocampus

Introduction

Given that selectively increasing liver-derived systemic concentrations of Gpld1 is sufficient to improve adult neurogenesis and cognitive function in the aged hippocampus, we next sought to delineate how Gpld1 exerts these effects. In its canonical role, Gpld1 hydrolyzes GPI anchors that have acylated inositol, releasing membrane bound GPI-anchored proteins from the cell surface(*149-152*). Although the physiological role of Gpld1 is not fully understood, cleavage of its substrates regulates signaling cascades important in biological processes such as differentiation and inflammation(*151*, *153*). Inflammatory cascades have previously been implicated in aging processes(*20*, *154*, *155*), positing Gpld1 as a potential modulator of the aging systemic milieu. We therefore sought to determine if Gpld1 was functioning primarily in the periphery or central nervous system, and characterize the signaling cascades downstream of its function. We hypothesized that that Gpld1-mediated GPI-anchor hydrolysis recapitulates changes in the aging systemic milieu to increase regenerative and cognitive function in the aged brain.

Results

Gpld1 does not readily cross the blood brain barrier

We sought to delineate central versus peripheral mechanisms of action of liver-derived Gpld1. To evaluate the potential of Gpld1 to cross the blood-brain-barrier we generated expression constructs encoding a high affinity nanoluciferase binary technology (HiBiT)-tagged version of Gpld1 (**Figure 6.1 A**). HiBiT is a small peptide with high affinity to large BiT (LgBiT) with which it forms a complex that produces a luminescent signal(*156*), allowing for sensitive and quantitative detection of tagged proteins. Aged mice were given HDTVI with expression constructs encoding HiBiT Gpld1, which we detected in plasma (**Figure 6.1 B**). We characterized HiBiT activity in mice in plasma, liver, cortex, hippocampus and cerebellum (**Figure 6.1 B-C**). Luminescent signal was detected in plasma and liver (**Figure 6.1 B-C**). However, the signal detected in the brain (**Figure 6.1 C**) was several orders of magnitude lower than that in plasma. Thus liver-derived systemic Gpld1 appears not to readily enter the brain.

Gpld1 alters systemic signaling cascades downstream of GPI-anchored substrate cleavage

As Gpld1 canonically functions through cleavage of GPI-anchored substrates, we next measured relative amounts of soluble proteins in the plasma of aged mice given HDTVI with expression constructs encoding Gpld1 or GFP control by label-free mass spectrometry. We surveyed the top 20 up- and down-regulated proteins (**Figure 6.2 A**) for known signaling cascades associated with Gpld1 substrates(*151*), and detected changes in the urokinase-type plasminogen activator receptor (uPAR) signaling pathway. uPAR is a Gpld1 GPI-anchored substrate, whose proteolytic function regulates the plasminogen (Plg) activation system involved in coagulation. Non-proteolytic function of uPAR regulates extracellular matrix proteins through interactions with Vitronectin (Vtn)(*153, 157*). On Western blots, we observed decreased amounts of both Plg and

Vtn in plasma of aged animals with increased systemic Gpld1 compared to those from control animals (**Figure 6.2 B-C**). We surveyed our previous exercise proteomic analysis for proteins that decrease in plasma of aged mice after exercise and also identified Plg (**Figure 6.2 D**). We compared functional enrichment analysis using STRING of factors identified to decrease in aged plasma following either Gpld1 overexpression (**Figure 6.2 A**) or exercise (**Figure 6.2 D**). Consistent with changes in the uPAR signaling pathway, we identified biological processes involved in coagulation, as well as the complement system, under both conditions (**Figure 6.2 E-F**). Of the factors surveyed after increased systemic Gpld1 and exercise, we identified 80% and 71% respectively, to be predominantly expressed in the liver according to Tabula Muris(*145*) and the protein atlas(*146*). Together, systemic changes in signaling cascades downstream of GPI-anchored substrate cleavage correlate with beneficial effects of Gpld1 and exercise.

GPI-anchored substrate cleavage is associated with restorative effects of Gpld1

We tested whether the enzymatic activity of liver-derived systemic Gpld1, and presumed subsequent GPI-anchored substrate cleavage, directly mediates its effects on adult neurogenesis and cognitive function in the aged hippocampus. The catalytic activity of Gpld1 is dependent on histidines at position 133 and 158, and mutations in either site abrogate enzymatic activity(*158*). We generated expression constructs encoding Gpld1 with site-directed mutations converting histidine into asparagine, and abrogation of GPI-anchored substrate cleavage was validated *in vitro* (**Figure 6.3 A**). Aged mice were injected with expression constructs encoding either Gpld1, catalytically inactive H133N Gpld1 or GFP control (**Figure 6.3 B**), and plasma concentrations were measured (**Figure 6.3 C**). We observed increased adult neurogenesis (**Figure 6.3 D**), increased BDNF expression (**Figure 6.3 E**), and cognitive improvements in the RAWM and novel object recognition tasks (**Figure 6.3 F-H**) in aged mice with increased expression of Gpld1. However, no differences were observed in aged mice with increased expression of catalytically inactive H133N Gpld1(**Figure 6.3 D-H**). These data indicate that the enzymatic activity of liver-

derived systemic Gpld1 is necessary for its effects on the aged hippocampus, and are consistent

with signaling cascades activated after of GPI-anchored substrate cleavage as possible molecular

mediators of these beneficial effects.
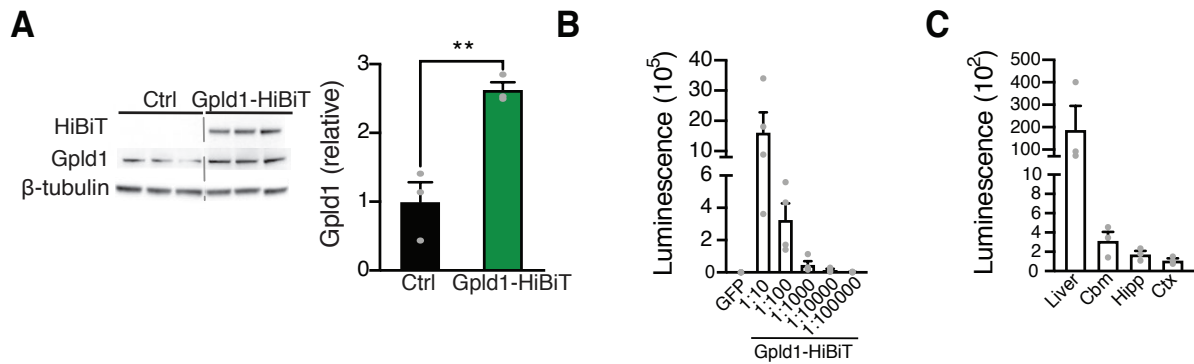
Figure 6.1. Assessment of Gpld1 localization. (**A**) Western blot and quantification of Gpld1 and HiBiT following transfection of control (GFP) or HiBiT-tagged Gpld1 (Gpld1-HiBiT) constructs in 293T cells *in vitro*. (n = 3 per group) (**B**-**C**) Aged (23 months) mice were given hydrodynamic tail vein injections (HDTVI) of expression constructs encoding either Gpld1, Gpld1-HiBiT, or GFP control. Luminescence-based quantification of Gpld1-HiBiT in serial dilutions of blood plasma (**B**) or tissues (**C**) from aged mice following HDTVI (n = 3-4 per group). All data are shown as mean±s.e.m; **P<0.01; *t* test (**A**).

A

B

C

D Decrease in Aged + Exercise

Serpina10	F2	C5	Hpx
Serpind1	Serpinf1	Cfi	Cd5l
Hspa5	Plg	Cfh	Fgb
Apoa4	F9	Itih4	Krt42
Fn1	Azgp1	Fgg	Orm1
Mbl1	Pvalb	Qsox1	Cfp
F13a1	Vcam1	C1sa	C9
Agt	Cp	Fga	Cfb
Gc	Cpb2	Actb	Orm2
Olfm1	C4b	Serpina3n	Saa1
			Hp

E Biological Processes: Gpld1

F Biological Processes: Aged + Exercise
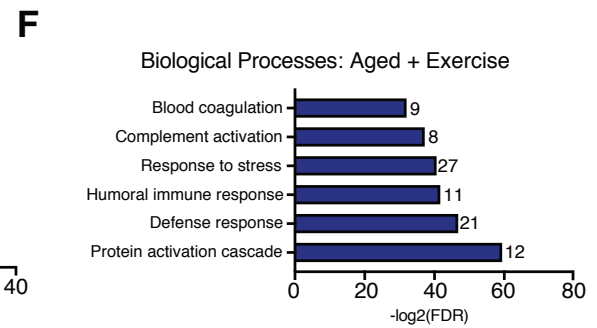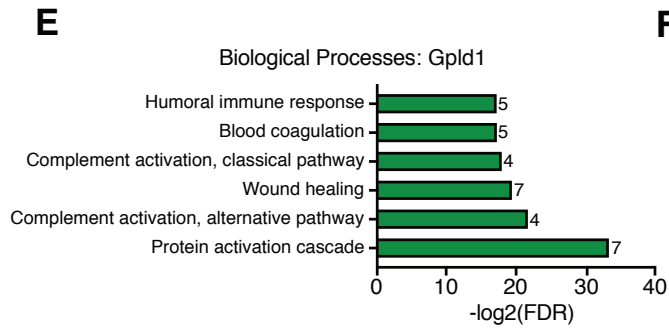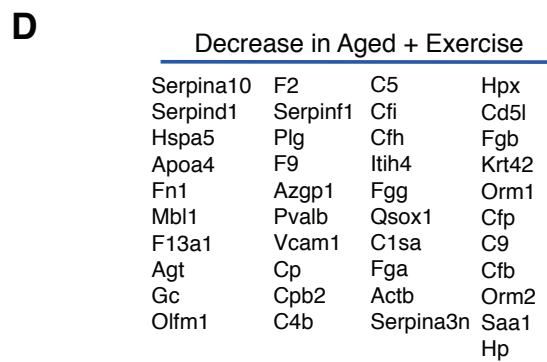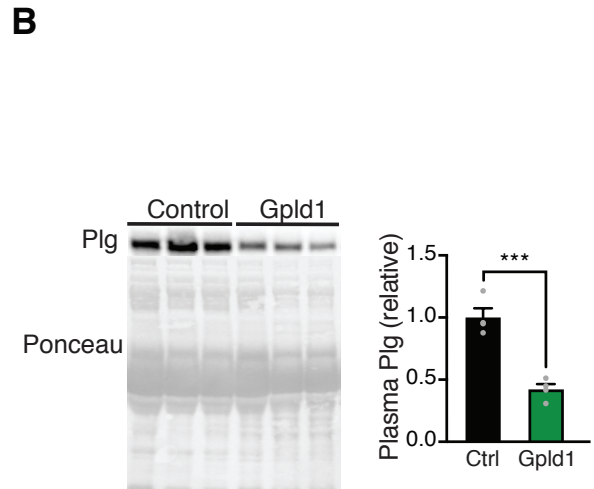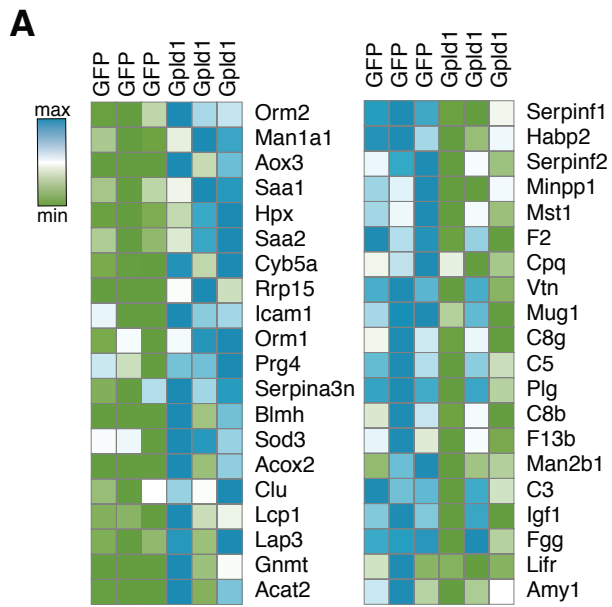
Figure 6.2. **Increased systemic Gpld1 alters signaling cascades downstream of GPI-anchored substrate cleavage in the aging systemic milieu.** (**A**) Heatmaps of top 20 proteins up- and down-regulated in blood plasma of aged mice following Gpld1 HDTVI compared to GFP HDTVI control, identified by mass spectrometry. (**B-C**) Western blot with corresponding Ponceau S stain and quantification of plasminogen (Plg; **B**) and vitronectin (Vtn; **C**) in equal volumes of blood plasma from individual aged mice 24 hours after HDTVI of Gpld1 or GFP control (n=4 per group). (**D**) List of 41 proteins downregulated in blood plasma from aged mice following exercise. (**E,F**) Enrichment analysis of plasma proteins downregulated with Gpld1 HDTVI (**E**) or exercise (**F**) in aged mice identified by mass spectrometry. The number of proteins represented in each process is listed to the right of each bar. All data are shown as mean±s.e.m.; **P<0.01, ***P<0.001; *t* test (**B, C**).
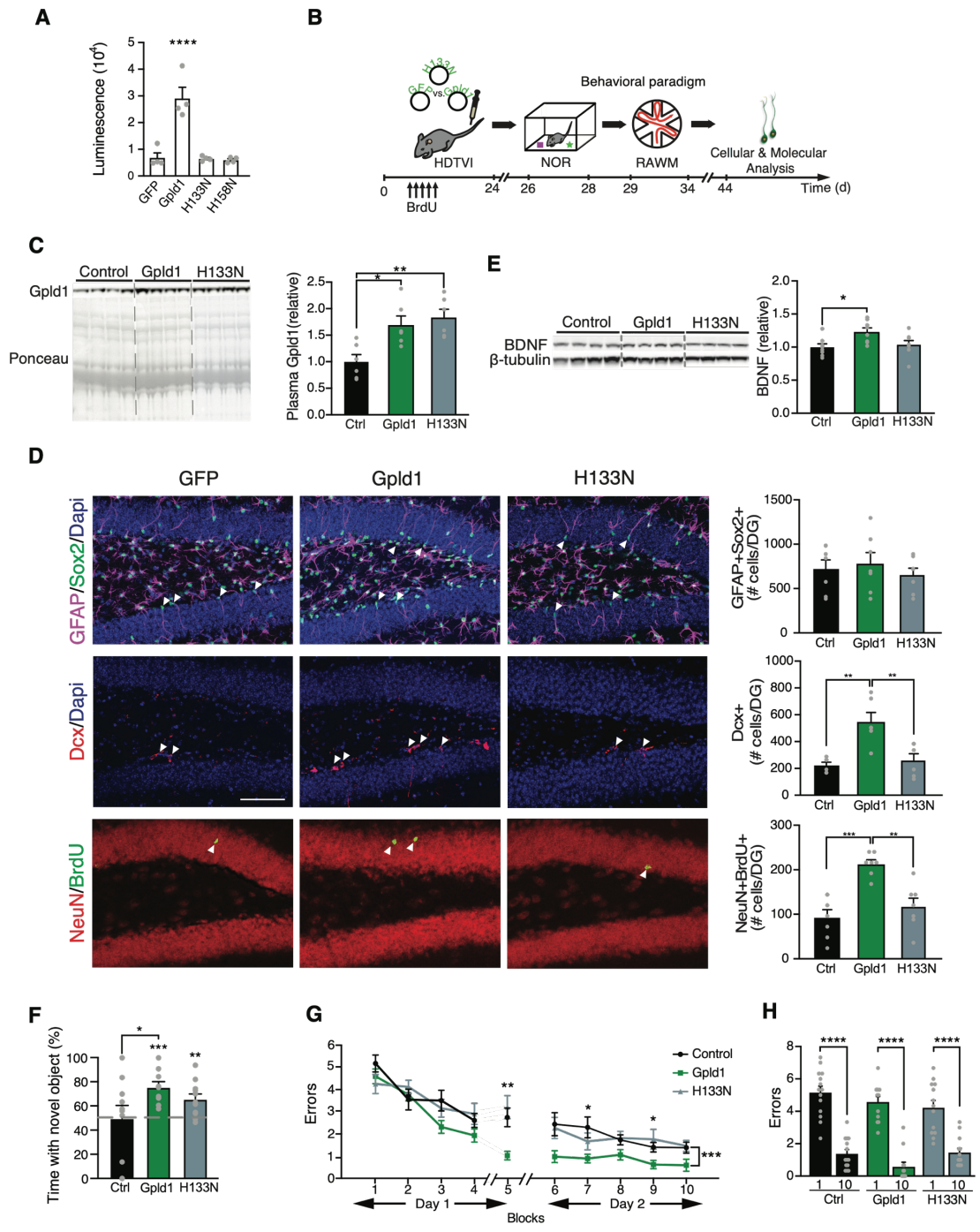
Figure 6.3. GPI-anchored substrate cleavage is associated with restorative effects of Gpld1 on the aged hippocampus. (**A**) Luminescence-based quantification of alkaline phosphatase activity in cell culture supernatant 48 hours after transfection with Ubiquitin-lox-stop-lox-PLAP (GPI-anchored alkaline phosphatase) and EF1a-Cre, in combination with either: CMV-GFP, CMV-Gpld1, CMV-H133N-Gpld1, or CMV-H158N-Gpld1 (n=3 samples/group). (**B**) Aged (18 months) mice were given hydrodynamic tail vein injections (HDTVI) of expression constructs encoding either Gpld1, catalytically inactive H133N-Gpld1, or GFP control. Schematic illustrates chronological order of HDTVI, cognitive testing, and cellular and molecular analysis. (**C**) Western blot with corresponding Ponceau S stain and quantification of Gpld1 in equal volumes of blood plasma from individual aged mice expressing Gpld1, Gpld1-H133N, or GFP control (n=6 per group). (**D**) Representative field and quantification of GFAP/Sox2 double-positive, Dcx-positive, and NeuN/BrdU double-positive cells in the DG of the hippocampus of aged mice expressing Gpld1, Gpld1-H133N, or GFP control (n=7 per group; Arrowheads point to individual cells; scale bar 100µm). (**E**) Western blot and quantification of BDNF in the hippocampus of aged mice expressing Gpld1, Gpld1-H133N, or GFP control (n=8 per group). Quantification normalized to β-Tubulin. (**F**) Object recognition memory was assessed by Novel Object Recognition (NOR) as time spent exploring a novel object 24 hours after training (n=9-11 per group). (**G,H**) Spatial learning and memory were assessed by radial arm water maze (RAWM) as number of entry errors committed during the training and testing phases. Overall learning and memory was analyzed between Blo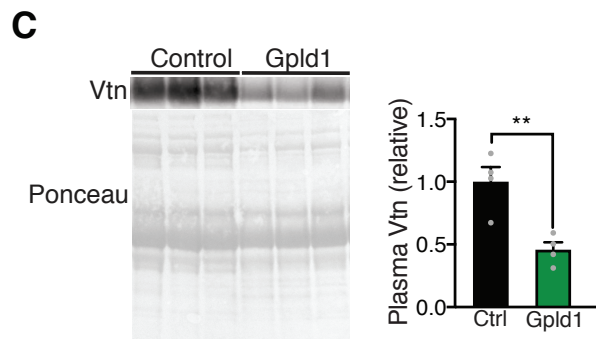ck 1 and 10 (1 Block = 3 Trials; n=12-14 per group). All data are shown as mean±s.e.m.; *$P<0.05$, **$P<0.01$, ***$P<0.001$, ****$P<0.0001$; repeated measures analysis of variance (ANOVA) with Bonferroni post-hoc test (**G**); ANOVA with Tukey's post-hoc test (**C-F, H**); One-sample *t* test versus 50% (**F**).

Discussion and Future Directions

Cumulatively, our data demonstrate that benefits of exercise on the aged brain can be transferred through administration of blood components. We identified the liver-derived factor Gpld1 as one such factor, and suspect that signaling cascades activated by GPI-anchored substrate cleavage activity may also participate. Our results identify a liver-to-brain axis by which circulating blood factors confer the beneficial effects of exercise in old age.

Adult neurogenesis in humans remains controversial(*23*). Nevertheless, adult neurogenesis is reported in the human hippocampus through the ninth decade of life, with age-related decline exacerbated in Alzheimer's disease (AD) patients(*25*) and correlating with cognitive dysfunction(*26*). In the context of dementia-related neurodegenerative diseases, exercise is correlated with reduced risk for cognitive decline in the elderly, improves cognition in populations at-risk for AD, and is associated with better neurobehavioral outcomes even in autosomal dominant AD(*106, 109, 159*). Exercise ameliorates impairments in learning and memory in animal models of AD(*118, 141*) by increasing adult neurogenesis and abundance of BDNF in the aged hippocampus(*118*) – benefits that we showed are transferred with injected plasma.

Our data identify decreased uPAR signaling - and associated changes in the coagulation and complement system cascades - as potential pro-aging molecular targets. The effects of liver-derived Gpld1 and exercise are likely the result of changes in multiple signaling cascades. However, a prominent role is emerging for the coagulation and complement pathways in aging. Changes in the coagulation pathway have been identified as part of the senescence-associated secretory phenotype (SASP)(*154*), and blood-derived complement C1q promotes age-related regenerative decline in peripheral tissues(*155*). The benefits of targeting members of the

coagulation pathway modulated by Gpld1 have been reported in the context of neurodegeneration(*160*). One of these members, Plg, is the zymogen of plasmin, which degrades fibrin and other extracellular matrix proteins to modulate a wide variety of cellular processes, including wound healing and cell migration (*161*). Genetic mouse models deficient for Plg were protected from demyelination and paralysis in a mouse model of multiple sclerosis(*161*). Moreover, targeting blood-derived Plg through oligonucleotide technologies decreased amyloid β plaque deposition and neuropathology in a mouse model of AD(*160*). Given that transfer of young blood simultaneously elicits central(*12*, *19*) and peripheral(*59*, *61*, *65*) enhancements in regenerative capacity in aged mice, our data raise the possibility that the beneficial effects of exercise could be promoted broadly across tissues through circulating blood factors.

References

1. C. López-Otin, M. A. Blasco, L. Partridge, M. Serrano, G. Kroemer, The Hallmarks of Aging. **153**, 1194–1217 (2013).

2. M. Mather, L. A. Jacobsen, K. M. Pollard, Aging in the United States. **70** (2015).

3. A. Association, 2016 Alzheimer's Disease Facts and Figures. **12** (2016).

4. T. Wyss-Coray, Ageing, neurodegeneration and brain rejuvenation. *Nature*. **539**, 180–186 (2016).

5. G. Neves, S. F. Cooke, T. V. P. Bliss, Synaptic plasticity, memory and the hippocampus: a neural network approach to causality. *Nature Reviews Neuroscience*. **9**, 65–75 (2008).

6. J. J. Knierim, The hippocampus. *Current Biology*. **25**, R1116–R1121 (2015).

7. A. Volianskis *et al.*, Long-term potentiation and the role of N-methyl-d-aspartate receptors. *Brain Res.* **1621**, 5–16 (2015).

8. M.-M. Poo *et al.*, What is memory? The present state of the engram. *BMC Biol*. **14**, 1–18 (2016).

9. A. M. Bond, G.-L. L. Ming, H. Song, Adult Mammalian Neural Stem Cells and Neurogenesis: Five Decades Later. *Cell Stem Cell*. **17**, 385–395 (2015).

10. A. Alvarez-Buylla, J. a-Verdugo, Neurogenesis in adult subventricular zone. *J Neurosci Official J Soc Neurosci*. **22**, 629–634 (2002).

11.   J. T. Gonçalves, S. T. Schafer, F. H. Gage, Adult Neurogenesis in the Hippocampus: From Stem Cells to Behavior. *Cell*. **167**, 897–914 (2016).

12.   X. Fan, E. G. Wheatley, S. A. Villeda, Mechanisms of Hippocampal Aging and the Potential for Rejuvenation. *Annu. Rev. Neurosci.* **40**, annurev–neuro–072116–031357 (2017).

13.   G.-L. Ming, H. Song, Adult Neurogenesis in the Mammalian Brain: Significant Answers and Significant Questions. *Neuron*. **70**, 687–702 (2011).

14.   G. Gontier *et al.*, Tet2 Rescues Age-Related Regenerative Decline and Enhances Cognitive Function in the Adult Mouse Brain. *Cell reports*. **22**, 1974–1981 (2018).

15.   V. M. Renault *et al.*, FoxO3 Regulates Neural Stem Cell Homeostasis. *Cell Stem Cell*. **5**, 527–539 (2009).

16.   A. V. Molofsky *et al.*, Bmi-1 dependence distinguishes neural stem cell self-renewal from progenitor proliferation. *Nature*. **425**, 962–967 (2003).

17.   C. Zhao, W. Deng, F. H. Gage, *Mechanisms and Functional Implications of Adult Neurogenesis. Cell 132* (2008).

18.   E. G. Waterhouse *et al.*, BDNF Promotes Differentiation and Maturation of Adult-born Neurons through GABAergic Transmission. *J. Neurosci.* **32**, 14318–14330 (2012).

19.   A. M. Horowitz, S. A. Villeda, Therapeutic potential of systemic brain rejuvenation strategies for neurodegenerative disease. *F1000Res*. **6**, 1291 (2017).

20.   S. A. Villeda *et al.*, The ageing systemic milieu negatively regulates neurogenesis and cognitive function. **477**, 90–94 (2011).

21.   A.-C. Dorsemans *et al.*, Diabetes, adult neurogenesis and brain remodeling: New insights from rodent and zebrafish models. *Neurogenesis*. **4**, e1281862 (2017).

22.   T. J. Schoenfeld, E. Gould, Stress, stress hormones, and adult neurogenesis. *Experimental Neurology*. **233**, 12–21 (2012).

23.   S. F. Sorrells *et al.*, Human hippocampal neurogenesis drops sharply in children to undetectable levels in adults. *Nature*. **555**, (2018).

24.   P. S. Eriksson *et al.*, Neurogenesis in the adult human hippocampus. *Nat. Med.* **4**, 1313–1317 (1998).

25.   E. P. Moreno-Jiménez *et al.*, Adult hippocampal neurogenesis is abundant in neurologically healthy subjects and drops sharply in patients with Alzheimer's disease. *Nature medicine*. **25**, 554–560 (2019).

26.   M. K. Tobin *et al.*, Human Hippocampal Neurogenesis Persists in Aged Adults and Alzheimer's Disease Patients. *Cell Stem Cell* (2019), doi:10.1016/j.stem.2019.05.003.

27.   K. L. Spalding *et al.*, Dynamics of Hippocampal Neurogenesis in Adult Humans. *Cell*. **153**, 1219–1227 (2013).

28.   M. Boldrini *et al.*, Human Hippocampal Neurogenesis Persists throughout Aging. *Cell Stem Cell*. **22**, 589–599.e5 (2018).

29.   J. H. Morrison, M. G. Baxter, The ageing cortical synapse: hallmarks and implications for cognitive decline. *Nature Reviews Neuroscience*. **13**, 240–250 (2012).

30.   E. Farkas, P. G. Luiten, Cerebral microvascular pathology in aging and Alzheimer's disease. *Prog. Neurobiol.* **64**, 575–611 (2001).

31.   J. R. Conde, W. J. Streit, Microglia in the aging brain. *J. Neuropathol. Exp. Neurol.* **65**, 199–203 (2006).

32.   H. G. Kuhn, H. Dickinson-Anson, F. H. Gage, Neurogenesis in the dentate gyrus of the adult rat: age-related decrease of neuronal progenitor proliferation. *J. Neurosci.* **16**, 2027–2033 (1996).

33.   L. Bondolfi, F. Ermini, J. M. Long, D. K. Ingram, Impact of age and caloric restriction on neurogenesis in the dentate gyrus of C57BL/6 mice. *Neurobiol. Aging.* **25**, 333–340 (2004).

34.   S. D. Kuipers, J. E. Schroeder, A. Trentani, Changes in hippocampal neurogenesis throughout early development. *Neurobiol. Aging.* **36**, 365–379 (2015).

35.   D. S. Leeman *et al.*, Lysosome activation clears aggregates and enhances quiescent neural stem cell activation during aging. *Science.* **359**, 1277–1283 (2018).

36.   D. R. Riddle, W. E. Sonntag, R. J. Lichtenwalner, Microvascular plasticity in aging. *Ageing Res. Rev.* **2**, 149–168 (2003).

37.   I. Soto *et al.*, APOE Stabilization by Exercise Prevents Aging Neurovascular Dysfunction and Complement Induction. *PLoS Biology.* **13**, e1002279 (2015).

38.   M. P. Mattson, T. Magnus, Ageing and neuronal vulnerability. *Nature Reviews Neuroscience.* **7**, 278–294 (2006).

39.   S. Hong *et al.*, Complement and microglia mediate early synapse loss in Alzheimer mouse models. *Science.* **352**, 712–716 (2016).

40.   A. Peters, C. Sethares, J. I. Luebke, Synapses are lost during aging in the primate

prefrontal cortex. *Neuroscience*. **152**, 970–981 (2008).

41.   D. A. Nicholson, R. Yoshida, R. W. Berry, M. Gallagher, Y. Geinisman, Reduction in
        size of perforated postsynaptic densities in hippocampal axospinous synapses and age-
        related spatial learning impairments. *J. Neurosci.* **24**, 7648–7653 (2004).

42.   O. von Bohlen und Halbach, C. Zacher, P. Gass, K. Unsicker, Age-related alterations in
        hippocampal spines and deficiencies in spatial memory in mice. *J. Neurosci. Res.* **83**,
        525–531 (2006).

43.   C. M. Alberini, Transcription factors in long-term memory and synaptic plasticity.
        Physiol. Rev. **89**, 121–145 (2009).

44.   E. S. Rosenzweig, C. A. Barnes, Impact of aging on hippocampal function: plasticity,
        network dynamics, and cognition. *Prog. Neurobiol.* **69**, 143–179 (2003).

45.   Y. Geinisman, Structural synaptic modifications associated with hippocampal LTP and
        behavioral learning. *Cereb. Cortex*. **10**, 952–962 (2000).

46.   E. Drapeau *et al.*, Spatial memory performances of aged rats in the water maze predict
        levels of hippocampal neurogenesis. *Proceedings of the National Academy of Sciences
        of the United States of America*. **100**, 14385–14390 (2003).

47.   D. A. Merrill, R. Karim, M. Darraq, A. A. Chiba, M. H. Tuszynski, Hippocampal cell
        genesis does not correlate with spatial learning ability in aged rats. *J. Comp. Neurol.*
        459, 201–207 (2003).

48.   S. Ge *et al.*, GABA regulates synaptic integration of newly generated neurons in the
        adult brain. *Nature*. **439**, 589–593 (2006).

49. S. Ge, C.-H. Yang, K.S. Hsu, G.L. Ming, H. Song, A Critical Period for Enhanced Synaptic Plasticity in Newly Generated Neurons of the Adult Brain. *Neuron*. **54**, 559–566 (2007).

50. N. Kee, C. M. Teixeira, A. H. Wang, P. W. Frankland, Preferential incorporation of adult-generated granule cells into spatial memory networks in the dentate gyrus. *Nat. Neurosci.* **10**, 355–362 (2007).

51. A. Sahay *et al.*, Increasing adult hippocampal neurogenesis is sufficient to improve pattern separation. *Nature*. **472**, 466–470 (2011).

52. W. Deng, M. D. Saxe, I. S. Gallina, F. H. Gage, Adult-born hippocampal dentate granule cells undergoing maturation modulate learning and memory in the brain. *J. Neurosci.* **29**, 13532–13542 (2009).

53. C. D. Clelland *et al.*, A functional role for adult hippocampal neurogenesis in spatial pattern separation. *Science*. **325**, 210–213 (2009).

54. Y. Gu *et al.*, Optical controlling reveals time-dependent roles for adult-born dentate granule cells. *Nat. Neurosci.* **15**, 1700–1706 (2012).

55. W. Deng, J. B. Aimone, F. H. Gage, New neurons and new memories: how does adult hippocampal neurogenesis affect learning and memory? *Nature Reviews Neuroscience*. **11**, 339–350 (2010).

56. G. Kempermann, The neurogenic reserve hypothesis: what is adult hippocampal neurogenesis good for? *Trends in neurosciences*. **31**, 163–169 (2008).

57. J. Bouchard, S. A. Villeda, Aging and brain rejuvenation as systemic events. *J Neurochem*. **132**, 5–19 (2015).

58.   F. S. Loffredo *et al.*, Growth Differentiation Factor 11 Is a Circulating Factor that Reverses Age-Related Cardiac Hypertrophy. *Cell*. **153**, 828–839 (2013).

59.   I. M. Conboy *et al.*, Rejuvenation of aged progenitor cells by exposure to a young systemic environment. *Nature*. **433**, 760–764 (2005).

60.   A. S. Brack *et al.*, Increased Wnt Signaling During Aging Alters Muscle Stem Cell Fate and Increases Fibrosis. *Science*. **317**, 807–810 (2007).

61.   M. Sinha *et al.*, Restoring systemic GDF11 levels reverses age-related dysfunction in mouse skeletal muscle. *Science*. **344**, 649–652 (2014).

62.   S. A. Villeda *et al.*, Young blood reverses age-related impairments in cognitive function and synaptic plasticity in mice. *Nat. Med.* **20**, 659–663 (2014).

63.   S. J. Salpeter *et al.*, Systemic Regulation of the Age-Related Decline of Pancreatic β-Cell Replication. *Diabetes*. **62**, 2843–2848 (2013).

64.   J. M. Ruckh *et al.*, Rejuvenation of regeneration in the aging central nervous system. *Cell Stem Cell*. **10**, 96–103 (2012).

65.   G. S. Baht *et al.*, Exposure to a youthful circulaton rejuvenates bone repair through modulation of β-catenin. *Nat Commun*. **6**, 7131 (2015).

66.   R. J. Colman *et al.*, Caloric Restriction Delays Disease Onset and Mortality in Rhesus Monkeys. *Science*. **325**, 201–204 (2009).

67.   R. J. Colman, T. M. Beasley, J. W. Kemnitz, Caloric restriction reduces age-related and all-cause mortality in rhesus monkeys. *Nature.* (2014).

68.   T. Samorajski *et al.*, Effect of exercise on longevity, body weight, locomotor

performance, and passive-avoidance memory of C57BL/6J mice. *Neurobiol. Aging*. **6**, 17–24 (1985).

69.   L. Katsimpardi *et al.*, Vascular and neurogenic rejuvenation of the aging mouse brain by young systemic factors. *Science*. **344**, 630–634 (2014).

70.   H. van Praag, T. Shubert, C. Zhao, F. H. Gage, Exercise enhances learning and hippocampal neurogenesis in aged mice. *J. Neurosci.* **25**, 8680–8685 (2005).

71.   M. W. Marlatt, M. C. Potter, P. J. Lucassen, H. van Praag, Running throughout middle-age improves memory function, hippocampal neurogenesis, and BDNF levels in female C57BL/6J mice. *Dev Neurobiol*. **72**, 943–952 (2012).

72.   R. Weindruch, R. L. Walford, Retardation of aging and disease by dietary restriction. *J Nutr*. (1988).

73.   J. Guo, V. Bakshi, A. L. Lin, Early Shifts of Brain metabolism by caloric restriction preserve white matter integrity and long-term memory in aging mice. *Frontiers in aging neuroscience* (2015).

74.   M. P. Mattson, Neuroprotective signaling and the aging brain: take away my food and let me run. *Brain research* (2000).

75.   M. Ferreira-Marques, C. A. Aveleira, Caloric restriction stimulates autophagy in rat cortical neurons through neuropeptide Y and ghrelin receptors activation. *Aging. (*2016).

76.   V. C. Cauwenberghe, C. Vandendriessche, Caloric restriction: beneficial effects on brain aging and Alzheimer's disease. *Mammalian Genome.* (2016).

77.   A. L. Lin, W. Zhang, X. Gao, L. Watts, Caloric restriction increases ketone bodies

metabolism and preserves blood flow in aging brain. *Neurobiology of aging* (2015).

78. I. Parikh *et al.*, Caloric restriction preserves memory and reduces anxiety of aging mice with early enhancement of neurovascular functions. *Aging*. **8**, 2814–2826 (2016).

79. N. Villain, J. L. Picq, F. Aujard, F. Pifferi, Body mass loss correlates with cognitive performance in primates under acute caloric restriction conditions. *Behavioural brain research* (2016).

80. A. Dal-Pan, F. Pifferi, J. Marchal, J. L. Picq, F. Aujard, Cognitive performances are selectively enhanced during chronic caloric restriction or resveratrol supplementation in a primate. *PloS one* (2011).

81. L. Ma *et al.*, Caloric restriction can improve learning ability in C57/BL mice via regulation of the insulin-PI3K/Akt signaling pathway. *Neurological Sci.* (2014).

82. S. M. Solon-Biet *et al.*, Defining the Nutritional and Metabolic Context of FGF21 Using the Geometric Framework. *Cell Metab.* **24**, 555–565 (2016).

83. S. A. Martin *et al.*, Regional metabolic heterogeneity of the hippocampus is nonuniformly impacted by age and caloric restriction. *Aging Cell*. **15**, 100–110 (2016).

84. A. Cardoso, F. Marrana, J. P. Andrade, Caloric restriction in young rats disturbs hippocampal neurogenesis and spatial learning. *Neurobio. of Learning and Memory*. **133**, 214–224 (2016).

85. C. Rühlmann, T. Wölk, T. Blümel, L. Stahn, Long-term caloric restriction in ApoE-deficient mice results in neuroprotection via Fgf21-induced AMPK/mTOR pathway. *Aging* (2016).

86. V. Halagappa, Z. Guo, M. Pearson, Y. Matsuoka, Intermittent fasting and caloric restriction ameliorate age-related behavioral deficits in the triple-transgenic mouse model of Alzheimer's disease. *Neurobiology of Disease.* (2007).

87. E. Ravussin *et al.*, A 2-Year Randomized Controlled Trial of Human Caloric Restriction: Feasibility and Effects on Predictors of Health Span and Longevity. *J. Gerontol. A Biol. Sci. Med. Sci.* **70**, 1097–1104 (2015).

88. L. K. Smith *et al.*, β2-microglobulin is a systemic pro-aging factor that impairs cognitive function and neurogenesis. *Nat. Med.* **21**, 932–937 (2015).

89. H. Yousef *et al.*, Aged blood impairs hippocampal neural precursor activity and activates microglia via brain endothelial cell VCAM1. *Nature medicine.* **25**, 988–1000 (2019).

90. J. Rebo *et al.*, A single heterochronic blood exchange reveals rapid inhibition of multiple tissues by old blood. *Nat Commun.* **7**, 13363 (2016).

91. H. Yousef *et al.*, Systemic attenuation of the TGF-β pathway by a single drug simultaneously rejuvenates hippocampal neurogenesis and myogenesis in the same old mammal. *Oncotarget.* **6**, 11959–11978 (2015).

92. M. Tavazoie *et al.*, A specialized vascular niche for adult neural stem cells. *Cell Stem Cell.* **3**, 279–288 (2008).

93. Q. Shen *et al.*, Endothelial cells stimulate self-renewal and expand neurogenesis of neural stem cells. *Science.* **304**, 1338–1340 (2004).

94. J. M. Castellano *et al.*, Human umbilical cord plasma proteins revitalize hippocampal function in aged mice. *Nature.* **544**, 488–492 (2017).

95.   M. A. Egerman *et al.*, GDF11 Increases with Age and Inhibits Skeletal Muscle Regeneration. *Cell Metabolism*. **22**, 164–174 (2015).

96.   A. Navarro, C. Gomez, Beneficial effects of moderate exercise on mice aging: survival, behavior, oxidative stress, and mitochondrial electron transfer. *Am J Physiol Regul Integr Comp Physiol* (2004).

97.   R. Garcia-Valles *et al.*, Life-long spontaneous exercise does not prolong lifespan but improves health span in mice. *Longev Healthspan*. **2**, 14 (2013).

98.   Q. L. Xue, The frailty syndrome: definition and natural history. *Clinics in geriatric medicine* (2011).

99.   R. B. Speisman, A. Kumar, A. Rani, T. C. Foster, B. K. Ormerod, Daily exercise improves memory, stimulates hippocampal neurogenesis and modulates immune and neuroimmune cytokines in aging rats. *Brain Behav. Immun.* **28**, 25–43 (2013).

100.   R. M. O'Callaghan, E. W. Griffin, A. M. Kelly, Long-term treadmill exposure protects against age-related neurodegenerative change in the rat hippocampus. *Hippocampus*. **19**, 1019–1029 (2009).

101.   J. Stessman, Physical Activity, Function, and Longevity Among the Very Old. *Arch Intern Med.* **169**, 1476 (2009).

102.   E. F. Chakravarty, Reduced Disability and Mortality Among Aging Runners. *Arch Intern Med.* **168**, 1638 (2008).

103.   L. H. Colbert, M. Visser, E. M. Simonsick, Physical activity, exercise, and inflammatory markers in older adults: findings from the Health, Aging and Body Composition Study. *American Geriatrics* (2004).

104.	M. A. Fiatarone, E. F. O'neill, N. D. Ryan, Exercise training and nutritional supplementation for physical frailty in very elderly people. *N Engl Journal of Medicine* (1994).

105.	N.J. Kirk-Sanchez, E.L. McGough, Physical exercise and cognitive performance in the elderly: current perspectives. *Clin Interv Aging* (2014).

106.	Y. E. Geda *et al.*, Physical exercise, aging, and mild cognitive impairment: a population-based study. *Arch. Neurol.* **67**, 80–86 (2010).

107.	S. Knecht, H. Wersching, H. Lohmann, M. Bruchmann, High-normal blood pressure is associated with poor cognitive performance. *Hypertension.* (2008).

108.	M. Fujishima, S. Ibayashi, K. Fujii, S. Mori, Cerebral blood flow and brain function in hypertension. *Hypertension Research* (1995).

109.	N. T. Lautenschlager *et al.*, Effect of physical activity on cognitive function in older adults at risk for Alzheimer disease: a randomized trial. *JAMA*. **300**, 1027–1037 (2008).

110.	R. E. Rhodes *et al.*, Factors associated with exercise adherence among older adults. An individual perspective. *Sports Med*. **28**, 397–411 (1999).

111.	S. F. Sleiman *et al.*, Exercise promotes the expression of brain derived neurotrophic factor (BDNF) through the action of the ketone body β-hydroxybutyrate. *Elife*. **5**, 560 (2016).

112.	S. Vaynman, Z. Ying, F. Gomez-Pinilla, Hippocampal BDNF mediates the efficacy of exercise on synaptic plasticity and cognition. *Eur. J. Neurosci.* **20**, 2580–2590 (2004).

113.	K. Fabel *et al.*, VEGF is necessary for exercise-induced adult hippocampal

neurogenesis. *Eur. J. Neurosci.* **18**, 2803–2812 (2003).

114.   R. A. Kohman *et al.*, Voluntary wheel running reverses age-induced changes in hippocampal gene expression. *Plos One*. **6**, e22654 (2011).

115.   E. Carro, A. Nuñez, S. Busiguina, I. Torres-Aleman, Circulating insulin-like growth factor I mediates effects of exercise on the brain. *J. Neurosci.* **20**, 2926–2933 (2000).

116.   J. L. Trejo, E. Carro, I. Torres-Aleman, Circulating Insulin-Like Growth Factor I Mediates Exercise-Induced Increases in the Number of New Neurons in the Adult Hippocampus. *J. Neurosci.* **21**, 1628–1634 (2001).

117.   F. G. Pinilla, S. Vaynman, Z. Ying, Brain-derived neurotrophic factor functions as a metabotrophin to mediate the effects of exercise on cognition. *European Journal of Neuroscience*. **28**, 2278–2287 (2008).

118.   S. H. Choi *et al.*, Combined adult neurogenesis and BDNF mimic exercise effects on cognition in an Alzheimer's mouse model. *Science*. **361**, eaan8821 (2018).

119.   H. Y. Moon *et al.*, Running-Induced Systemic Cathepsin B Secretion Is Associated with Memory Function. *Cell Metab*. **24**, 332–340 (2016).

120.   C. D. Wrann *et al.*, Exercise Induces Hippocampal BDNF through a PGC-1a/FNDC5 Pathway. *Cell Metabolism*. **18**, 649–659 (2013).

121.   O. Leiter *et al.*, Exercise-Induced Activated Platelets Increase Adult Hippocampal Precursor Proliferation and Promote Neuronal Differentiation. *Stem cell reports*. **12**, 667–679 (2019).

122.   M. V. Lourenco *et al.*, Exercise-linked FNDC5/irisin rescues synaptic plasticity and

memory defects in Alzheimer's models. *Nature medicine*. **25**, 165–175 (2019).

123. D. Kovacsics, J. Raper, Transient expression of proteins by hydrodynamic gene delivery in mice. *J Vis Exp* (2014).

124. J. Alamed, D. M. Wilcock, D. M. Diamond, M. N. Gordon, D. Morgan, Two-day radial-arm water maze learning and memory task; robust resolution of amyloid-related memory deficits in transgenic mice. *Nat Protoc*. **1**, 1671–1679 (2006).

125. K. Belarbi *et al.*, Beneficial effects of exercise in a transgenic mouse model of Alzheimer's disease-like Tau pathology. *Neurobiology of disease*. **43**, 486–494 (2011).

126. D. B. Dubal *et al.*, Life extension factor klotho prevents mortality and enhances cognition in hAPP transgenic mice. *J. Neurosci.* **35**, 2358–2371 (2015).

127. K. E. Williams *et al.*, Quantitative proteomic analyses of mammary organoids reveals distinct signatures after exposure to environmental chemicals. *Proceedings of the National Academy of Sciences of the United States of America*. **113**, E1343–51 (2016).

128. R. C. Dwivedi *et al.*, Practical implementation of 2D HPLC scheme with accurate peptide retention prediction in both dimensions for high-throughput bottom-up proteomics. *Anal. Chem.* **80**, 7036–7042 (2008).

129. W. H. Tang, I. V. Shilov, S. L. Seymour, Nonlinear fitting method for determining local false discovery rates from decoy database searches. *J. Proteome Res.* **7**, 3661–3667 (2008).

130. S. Tyanova, T. Temu, J. Cox, The MaxQuant computational platform for mass spectrometry-based shotgun proteomics. *Nat Protoc*. **11**, 2301–2319 (2016).

131. D. Szklarczyk *et al.*, STRING v11: protein-protein association networks with increased coverage, supporting functional discovery in genome-wide experimental datasets. *Nucleic Acids Res.* **47**, D607–D613 (2019).

132. V. J. Block *et al.*, Continuous daily assessment of multiple sclerosis disability using remote step count monitoring. *J. Neurol.* **264**, 316–326 (2017).

133. C. Tudor-Locke *et al.*, How many steps/day are enough? For older adults and special populations. *International Journal of Behavioral Nutrition and Physical Activity*. **8**, 80 (2011).

134. A. Kumar, A. Rani, O. Tchigranova, W.-H. Lee, T. C. Foster, Influence of late-life exposure to environmental enrichment or exercise on hippocampal function and CA1 senescent physiology. *Neurobiol. Aging*. **33**, 828.e1–17 (2012).

135. C.W. Wu *et al.*, Exercise enhances the proliferation of neural stem cells and neurite growth and survival of neuronal progenitor cells in dentate gyrus of middle-aged mice. *J Appl Physiol*. **105**, 1585–1594 (2008).

136. G. Kronenberg *et al.*, Physical exercise prevents age-related decline in precursor cell activity in the mouse dentate gyrus. *Neurobiol. Aging*. **27**, 1505–1513 (2006).

137. S. Lugert *et al.*, Quiescent and Active Hippocampal Neural Stem Cells with Distinct Morphologies Respond Selectively to Physiological and Pathological Stimuli and Aging. *Cell Stem Cell*. **6**, 445–456 (2010).

138. T. E. Gibbons *et al.*, Voluntary wheel running, but not a diet containing (-)-epigallocatechin-3-gallate and β-alanine, improves learning, memory and hippocampal neurogenesis in aged mice. *Behavioural brain research*. **272**, 131–140 (2014).

139.   K. I. Erickson *et al.*, Exercise training increases size of hippocampus and improves memory. *Proceedings of the National Academy of Sciences of the United States of America*. **108**, 3017–3022 (2011).

140.   A. Maass *et al.*, Vascular hippocampal plasticity after aerobic exercise in older adults. *Mol. Psychiatry*. **20**, 585–593 (2015).

141.   K. A. Intlekofer, C. W. Cotman, Exercise counteracts declining hippocampal function in aging and Alzheimer's disease. *Neurobiology of disease* (2013).

142.   H. van Praag, B. R. Christie, T. J. Sejnowski, F. H. Gage, Running enhances neurogenesis, learning, and long-term potentiation in mice. *Proceedings of the National Academy of Sciences of the United States of America*. **96**, 13427–13431 (1999).

143.   D. J. Creer, C. Romberg, L. M. Saksida, H. van Praag, T. J. Bussey, Running enhances spatial pattern separation in mice. *Proceedings of the National Academy of Sciences of the United States of America*. **107**, 2367–2372 (2010).

144.   L. K. Smith *et al.*, The aged hematopoietic system promotes hippocampal-dependent cognitive decline. *Aging Cell*. (2020).

145.   Tabula Muris Consortium *et al.*, Single-cell transcriptomics of 20 mouse organs creates a Tabula Muris. *Nature*. **562**, 367–372 (2018).

146.   M. Uhlén *et al.*, Proteomics. Tissue-based map of the human proteome. *Science*. **347**, 1260419–1260419 (2015).

147.   B. J. Scallon *et al.*, Primary structure and functional activity of a phosphatidylinositol-glycan-specific phospholipase D. *Science*. **252**, 446–448 (1991).

148.   G. A. Maguire, A. Gossner, Glycosyl phosphatidyl inositol phospholipase D activity in human serum. *Ann. Clin. Biochem.* **32 (Pt 1)**, 74–78 (1995).

149.   M. A. Davitz *et al.*, A glycan-phosphatidylinositol-specific phospholipase D in human serum. *Science*. **238**, 81–84 (1987).

150.   C. N. Metz *et al.*, Release of GPI-anchored membrane proteins by a cell-associated GPI-specific phospholipase D. *EMBO J.* **13**, 1741–1751 (1994).

151.   Y. Fujihara, M. Ikawa, GPI-AP release in cellular, developmental, and reproductive biology. *Journal of lipid research*. **57**, 538–545 (2016).

152.   M. G. Low, A. R. S. Prasad, A phospholipase D specific for the phosphatidylinositol anchor of cell-surface proteins is abundant in plasma. *Proceedings of the National Academy of Sciences*. **85**, 980–984 (1988).

153.   M. Del Rosso *et al.*, The urokinase receptor system, a key regulator at the intersection between inflammation, immunity, and coagulation. *Curr. Pharm. Des.* **17**, 1924–1943 (2011).

154.   C. D. Wiley *et al.*, SILAC Analysis Reveals Increased Secretion of Hemostasis-Related Factors by Senescent Cells. *Cell reports*. **28**, 3329–3337.e5 (2019).

155.   A. T. Naito *et al.*, Complement C1q activates canonical Wnt signaling and promotes aging-related phenotypes. *Cell*. **149**, 1298–1313 (2012).

156.   M. K. Schwinn *et al.*, CRISPR-Mediated Tagging of Endogenous Proteins with a Luminescent Peptide. *ACS Chem. Biol.* **13**, 467–474 (2018).

157.   F. Blasi, N. Sidenius, The urokinase receptor: focused cell surface proteolysis, cell

adhesion and signaling. *FEBS Lett.* **584**, 1923–1930 (2010).

158.   N. S. Raikwar, R. F. Bowen, M. A. Deeg, Mutating His29, His125, His133 or His158 abolishes glycosylphosphatidylinositol-specific phospholipase D catalytic activity. *Biochem. J.* **391**, 285–289 (2005).

159.   S. Müller *et al.*, Relationship between physical activity, cognition, and Alzheimer pathology in autosomal dominant Alzheimer's disease. *Alzheimers Dement*. **14**, 1427–1437 (2018).

160.   S. K. Baker *et al.*, Blood-derived plasminogen drives brain inflammation and plaque deposition in a mouse model of Alzheimer's disease. *Proceedings of the National Academy of Sciences of the United States of America*. **115**, E9687–E9696 (2018).

161.   M. A. Shaw *et al.*, Plasminogen Deficiency Delays the Onset and Protects from Demyelination and Paralysis in Autoimmune Neuroinflammatory Disease. *J. Neurosci.* **37**, 3776–3788 (2017).

Publishing Agreement

It is the policy of the University to encourage open access and broad distribution of all theses, dissertations, and manuscripts. The Graduate Division will facilitate the distribution of UCSF theses, dissertations, and manuscripts to the UCSF Library for open access and distribution. UCSF will make such theses, dissertations, and manuscripts accessible to the public and will take reasonable steps to preserve these works in perpetuity.

I hereby grant the non-exclusive, perpetual right to The Regents of the University of California to reproduce, publicly display, distribute, preserve, and publish copies of my thesis, dissertation, or manuscript in any form or media, now existing or later derived, including access online for teaching, research, and public service purposes.

DocuSigned by:

Alana Horowitz

—— 3B1E53C97707431...

Author Signature

8/12/2020

Date